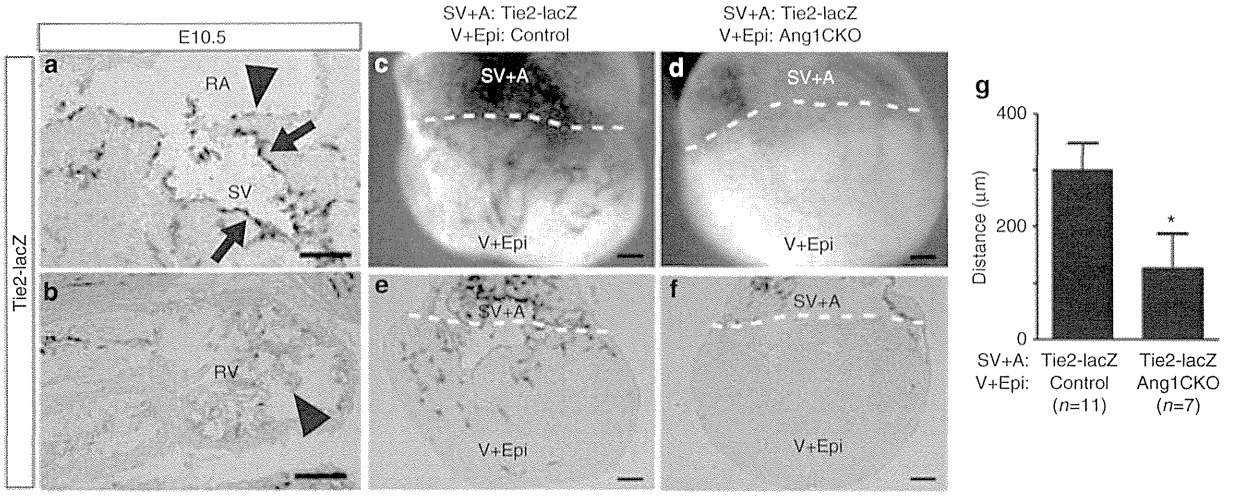

Figure 5 | Ang1 derived from the ventricular myocardium attracts Tie2-positive ECs from the SV. (**a**,**b**) X-gal staining of *Tie2-lacZ* transgenic mice at E10.5. Tie2-positive signals were observed most strongly in the SV (arrows), and to a much lesser extent in the endocardium of both the RA and RV (arrowheads). (**c**–**f**) Analysis of coronary vessel sprouting *in vitro*. The SV and atrium (SV + A) resected from *Tie2-LacZ* transgenic embryos were recombined with the ventricle and epicardium (V + Epi) resected from either control or Ang1CKO embryos at E10.5, cultured for 72 h at 37 °C, and subjected to whole-mount staining with X-gal (**c**,**d**). Tie2-lacZ-positive coronary sprouts formed when recombined with the V + Epi from control (**c**), but not with the V + Epi from Ang1CKO embryos (**d**). Whole-mount X-gal-stained samples were sectioned (**e**,**f**). The migratory distances from the combined atrioventricular borderline (dotted line) to the forefront of the Tie2-lacZ-positive signals in the ventricles were measured. The mean migratory distance of each group is shown in **g**. Scale bars, 100 μm. A, atrium; Epi, epicardium; RV, right ventricle; SV, sinus venosus; V, ventricle. Values are shown as means ± s.e.m.. Student's *t*-test was used to analyse differences. $^*P<0.05$ compared with control.

Tie2-lacZ-positive signals were observed in the atria or ventricle in a similar patchy fashion (Supplementary Fig. 6c,d).

The SV + A resected from *Tie2-lacZ* transgenic mice were combined with the V + Epi resected from either control or Ang1CKO mice, and then cultured for 72 h and stained with X-gal to determine whether Tie2-lacZ-positive coronary vessels had sprouted and migrated into the ventricles (Fig. 5). When the SV + A resected from *Tie2-lacZ* mice was cultured with the V + Epi of control mice, Tie2-lacZ-positive coronary vessels were detected on the V + Epi (Fig. 5c,e; 7 of 11, 64%). However, when the SV + A resected from *Tie2-lacZ* mice were cultured with the V + Epi of Ang1CKO mice, the formation of Tie2-lacZ-positive coronary vessels on the V + Epi was disturbed (Fig. 5d,f; 2 of 7, 29%). Consistent with these findings, the mean migratory distance from the border between the atrium and ventricle to the leading edge of the Tie2-positive ECs in the ventricle was significantly longer in the culture of the *Tie2-lacZ* atrium with the control ventricle than in that of the *Tie2-lacZ* atrium with the Ang1CKO ventricle (Fig. 5g). Collectively, these experiments suggest that Ang1 derived from the ventricular myocardium might be involved in attraction of the Tie2-positive ECs from the SV towards the ventricular myocardium.

The ECs of SV consist of APJ-positive and APJ-negative cells. The SV is considered one of the most plausible sites of origin for coronary vein ECs[9,11]. Therefore, we examined the expression patterns of several EC markers in the SV. We performed double immunostaining with anti-CD31 and anti-Tie2 antibodies. Consistent with the results obtained from the X-gal staining of *Tie2-lacZ* transgenic mice, all of the CD31-positive ECs in the SV were positive for Tie2 in control embryos (Fig. 6a–c). Furthermore, the expression pattern of Tie2 in Ang1CKO and control embryos was quite similar (Fig. 6d–f), suggesting that Tie2 is uniformly expressed in the ECs of the SV in both control and Ang1CKO embryos. In addition, VEGFR2 immunostaining colocalized with that of Tie2 in the SV of control and Ang1CKO embryos (Supplementary Fig. 7a–f), indicating that VEGFR2 is also uniformly expressed in the ECs of the SV. We also performed X-gal staining of *EphrinB2-lacZ* knockin mice at E10.5 and confirmed that the arterial endothelial marker EphrinB2 is not expressed in the SV at E10.5 (Supplementary Fig. 7g–i). These data suggest that CD31, Tie2 and VEGFR2 are all expressed uniformly in the ECs of the SV.

In clear contrast, APJ was not uniformly expressed in the ECs of the SV in either control or Ang1CKO embryos (Fig. 6g–l). This finding indicates that the ECs in the SV at E10.5 consist of two populations, namely the APJ-positive and APJ-negative ECs (Fig. 6m).

The APJ-negative ECs migrate from SV into myocardium. We next addressed the characteristics of the CD31-positive ECs migrating from the SV into the atrium. Intriguingly, APJ-negative ECs were exclusively detected in the coronary sprouts in the atria of both control and Ang1CKO embryos at E11.5 (Fig. 6n–t). We also confirmed that APJ-positive vessels were not detected in the atrium of either control or Ang1CKO embryos at E11.5 by whole-mount immunostaining with an anti-APJ antibody (Supplementary Fig. 7j–m). However, at E12.5, APJ was expressed in the atrial CD31-positive vessels in control embryos, but not in Ang1CKO embryos (Fig. 6u–z, arrowheads). These data are consistent with the data obtained from whole-mount immunostaining with the anti-APJ antibody at E13.0 (Fig. 2a,b). Taken together, these findings suggest that Ang1 secreted from the atrial myocardium promotes the upregulation of APJ and the venous differentiation of ECs sprouting from the SV into the atrium of control embryos (Fig. 6aa).

The expression of APJ in the vessels migrating from the atrium into the ventricles was not detected in control or Ang1CKO embryos at E12.5 (Fig. 6u–z, arrow). These data indicate that the APJ-negative ECs migrate from the SV into the atrium at E11.5

(Fig. 6t) and subsequently into the ventricle at E12.5, followed by the appearance of APJ-positive, mature ECs in the atrium (Fig. 6aa). Whole-mount immunostaining analysis of the wild-type embryos revealed the emergence of APJ-positive vessels on the ventricular surface on and after E13.5 (Supplementary Fig. 2e–h), one day later than the emergence of CD31-positive vessels (Supplementary Fig. 2a–d). These findings indicate that the APJ-negative ECs precede the appearance of the APJ-positive mature venous ECs in the ventricle.

The APJ-negative ECs were also detected in the ventricles of wild-type embryos both at E12.5 (Fig. 7a–c, j, arrows in area 2) and E13.5 (Fig. 7d–f, k, arrows in area 4). However, at E14.5, the APJ-negative subepicardial ECs could not be detected at the forefront of the invading vessels in the wild-type ventricles (Fig. 7g–i, l). These data suggest that immature APJ-negative ECs in the ventricles may differentiate into APJ-positive ECs at E14.5 in response to myocardial Angl (Fig. 7l).

Consistent with the whole-mount immunostaining with anti-APJ antibody results (Fig. 2c,d,g,h), APJ-positive ECs were observed in the basal subepicardial layers of both the right and left ventricles of control embryos, but not in those of Ang1CKO embryos at E13.5 (Supplementary Fig. 8a–g). Taken together, these data suggest that the APJ-negative ECs migrate from the SV into the atrium and subsequently into the ventricle at the forefront of the invading vessels and precede the appearance of APJ-positive ECs. The emergence of APJ-positive ECs occurs one day later in the atria and ventricles and requires the presence of myocardial Angl.

In addition, we examined the proliferation of the subepicardial CD31-positive ECs in the hearts of both control and Ang1CKO embryos. Since we observed the invasion of CD31-positive subepicardial ECs from atria into the basal region of the ventricles in both control and Ang1CKO embryos (Fig. 1e,f), we examined the proliferation of CD31-positive subepicardial ECs in the ventricles of control and Ang1CKO embryos. The number of subepicardial ECs double-positive for pHH3 and CD31 in the ventricles of Ang1CKO embryos was 44% smaller than that in control embryos (Supplementary Fig. 9a–c), suggesting that myocardial deletion of Angl led to the impaired proliferation of CD31-positive subepicardial ECs.

We also examined the expression levels of *VEGF-A* and *VEGFR2* mRNAs in the hearts. They were almost comparable between control and Ang1CKO embryos (Supplementary Fig. 9d,e), indicating that the CD31-positive APJ-negative immature ECs in the subepicardial region of Ang1CKO hearts might be recruited from SV partly by the action of myocardium-derived VEGF-A. These findings suggest that myocardial Angl contributes not only to the migration but also to the proliferation of subepicardial immature ECs.

Angl promotes venous differentiation of the immature ECs. The finding that APJ-negative ECs of the SV expressed APJ one or two days after migrating into the myocardium in control mice, but not in Ang1CKO mice suggested that Angl might be critically involved in the venous differentiation of immature ECs in the heart. Therefore, we examined the effect of Angl on arterial–venous specification using the Flk1-positive endothelial progenitor cells derived from embryonic stem (ES) cells (Flk1$^+$ cells)[28,31]. Since the ECs that invade the atrium from the SV do not express either the arterial marker EphrinB2 or the venous marker APJ, we reasoned that the Flk1$^+$ cells, which are double-negative for these markers, would be suitable for analysing the effects of Angl on the arterial–venous specification of the ECs. Treatment with VEGF and 8-bromo-cyclic-AMP (cAMP) upregulated the expression of the arterial marker EphrinB2 in Flk1$^+$ cells, as reported previously (Supplementary Fig. 10a,b)[31]. Next, we examined the additive effects of treatment with cartilage oligomeric matrix protein (COMP)-Angl, a potent variant of Angl (ref. 32), VEGF and cAMP on Flk1$^+$ cells. Interestingly, treatment with COMP-Angl inhibited the induction of EphrinB2 by VEGF and cAMP (Supplementary Fig. 10c). qRT–PCR analysis also demonstrated that co-treatment with COMP-Angl counteracted the upregulation of *Efnb2* mRNA by VEGF and cAMP (Supplementary Fig. 10d).

In contrast, immunocytochemical analysis revealed that the transcription factor COUP-TFII, which is postulated to have a key role in venous differentiation[24,25], was significantly upregulated in Flk1$^+$ cells when stimulated with VEGF, cAMP and COMP-Angl (Fig. 8a–c). Consistent with these findings, qRT–PCR analysis revealed that co-stimulation with VEGF, cAMP and COMP-Angl upregulated the expression level of *COUP-TFII* in Flk1$^+$ cells, although neither the co-stimulation with VEGF and cAMP nor that with VEGF and Angl upregulated the expression level of *COUP-TFII* (Fig. 8d).

Interestingly, co-stimulation with VEGF and COMP-Angl did upregulate the expression level of *APJ* mRNA in Flk1$^+$ cells, whereas VEGF or co-stimulation with VEGF and cAMP did not significantly affect the expression level of *APJ*, indicating that APJ upregulation may be a prerequisite for the induction of COUP-TFII in Flk1$^+$ cells (Fig. 8e).

In addition, we also examined the requirement of Tie2 receptor for the effect of Angl on the venous differentiation of Flk1-positive endothelial progenitor cells by siRNA-mediated knockdown of Tie2. We first confirmed that the expression level of Tie2 protein was significantly reduced by approximately 80% in the immature Flk1-positive endothelial progenitor cells (Supplementary Fig. 11a). We found that siRNA-mediated knockdown of Tie2 significantly blunted Angl-dependent upregulation of *COUP-TFII* and *APJ* mRNAs (Supplementary Fig. 11b,c). These findings suggest that Tie2 activation is required for the Angl-dependent venous differentiation of the immature Flk1-positive endothelial progenitor cells. Collectively, these data suggest that Angl/Tie2 signalling promotes the venous differentiation of

Figure 6 | APJ-negative ECs sprout off from the SV and migrate into the embryonic atria and ventricles. (**a–f**) Sagittal section through the SV of control (**a–c**) and Ang1CKO embryos (**d–f**) at E10.5 immunostained for CD31 (green) and Tie2 (red). CD31 and Tie2 were uniformly expressed in the ECs of the SV (arrowheads). (**g–l**) Sagittal section through the SV of control (**g–i**) and Ang1CKO embryos (**j–l**) at E10.5 immunostained for CD31 (green) and APJ (red). APJ-negative ECs were detected among the CD31-positive ECs in both control and Ang1CKO embryos (arrows). ECs in the SV expressing both CD31 and APJ were similarly observed in control and Ang1CKO embryos (arrowheads). (**m**) Schematic illustrations of the SV at E10.5 showing that the ECs were heterogeneous for APJ expression. (**n–s**) Sagittal sections through the right atrium (RA) of control (**n–p**) and Ang1CKO embryos (**q–s**) at E11.5 immunostained for CD31 (green) and APJ (red). (**t**) Schematic illustrations of the RA at E11.5 showing that all of the invading ECs were negative for APJ in both control and Ang1CKO embryos. (**u–z**) Sagittal section through the RA and right ventricle (RV) of control (**u–w**) and Ang1CKO embryos (**x–z**) at E12.5 immunostained for CD31 (green) and APJ (red). The CD31-positive ECs invading the RV did not express APJ in either control or Ang1CKO embryos (arrow). In contrast, APJ was expressed in all of the CD31-positive ECs in the RA of control, but not Ang1CKO embryos (arrowheads). (**aa**) Schematic illustration of the RA and RV at E12.5 summarizing the expression of APJ. Blue line, APJ-positive ECs; black line, APJ-negative ECs. Scale bars, 50 μm. RA, right atrium; RV, right ventricle; SV, sinus venosus.

immature vascular progenitor Flk1^{+} cells via the upregulation of COUP-TFII and APJ. Since the growth factor(s) responsible for regulating COUP-TFII have not been identified to date, Ang1 might be a promising candidate factor for promoting the venous differentiation of immature ECs in the developing heart.

Discussion

These findings demonstrate that Ang1 is essential for coronary vein formation in developing heart (Fig. 9a,b). Ang1CKO mice displayed significant defects in the migration of the APJ-negative immature ECs from the SV into the myocardium, the proliferation and the venous differentiation of the immature ECs.

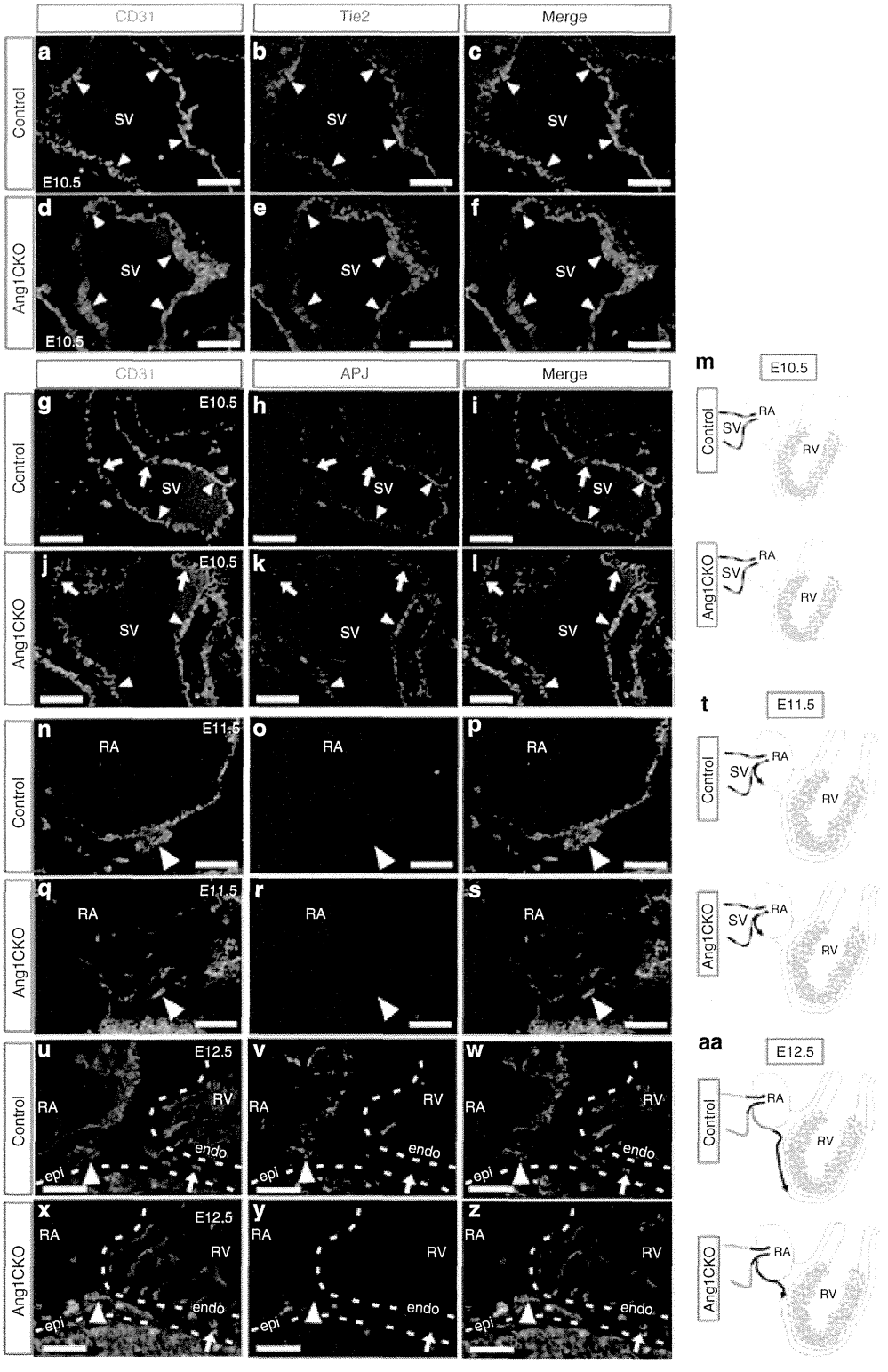

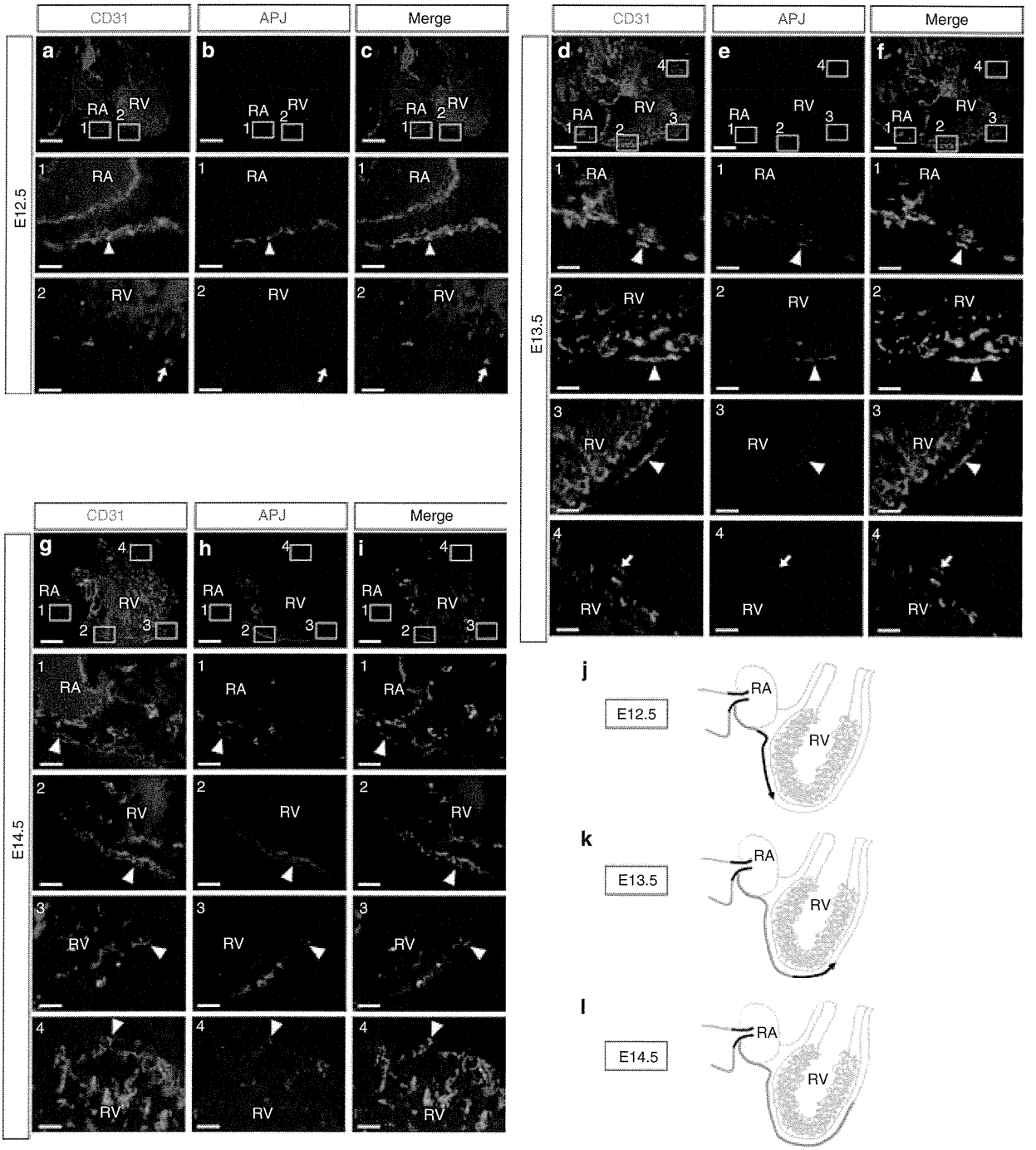

Figure 7 | APJ-negative ECs precede APJ-positive ECs on the ventricle surface. Sagittal sections through the RA and RV of wild-type embryos at E12.5 (**a**–**c**), E13.5 (**d**–**f**), E14.5 (**g**–**i**) immunostained for CD31 (green) and APJ (red). At E12.5 and E13.5, the APJ-negative (immature) ECs migrated at the forefront of the sprouting subepicardial coronary vessels (arrows in **a**–**c** area 2, **d**–**f** area 4) and preceded the appearance of the APJ-positive (mature) ECs (arrowheads). At E14.5, all of the subepicardial ECs were double-positive for CD31 and APJ (arrowheads in **g**–**i**). (**j**–**l**) Schematic illustration of the SV, RA and RV at E12.5 (**j**), E13.5 (**k**) and E14.5 (**l**). Blue line, APJ-positive ECs; black line, APJ-negative ECs. Scale bars, 200 μm (upper panels in **a**–**i**); 50 μm (insets). RA, right atrium; RV, right ventricle; SV, sinus venosus.

Together, Ang1CKO mice exhibited defective formation of subepicardial coronary veins. In addition, Ang1 in combination with VEGF and cAMP induced the venous differentiation of Flk1$^+$ vascular progenitor cells, whereas the combination of VEGF and cAMP promoted arterial differentiation of the Flk1$^+$ vascular progenitor cells. To our knowledge, this is the first report describing the growth factor responsible for the venous differentiation of immature ECs.

The origin of coronary ECs has been a long-lasting question. Ang1CKO mice displayed specific defects in the development of APJ-, EphB4-, COUP-TFII-positive coronary veins (Fig. 2); however, they showed no significant defects in coronary artery

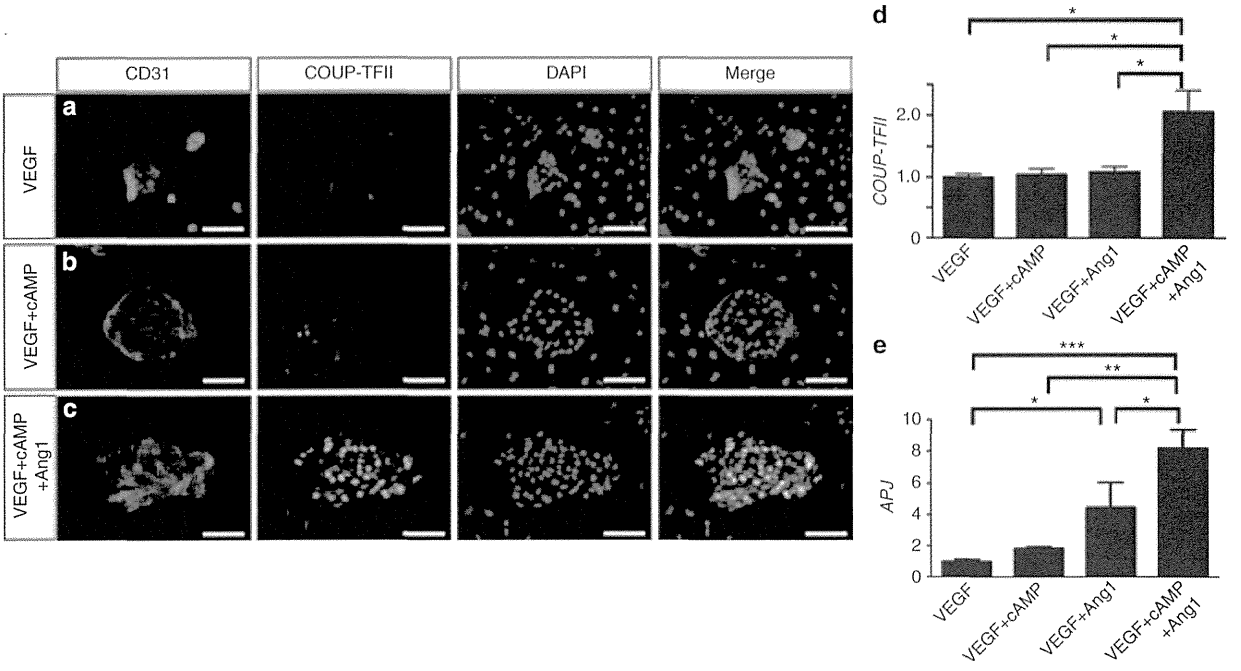

Figure 8 | Ang1 enhances venous differentiation of Flk1$^+$ immature endothelial progenitor cells synergistically with VEGF. (**a**–**c**) The venous marker protein COUP-TFII was upregulated in vascular progenitor Flk1$^+$ cells by the addition of COMP-Ang1 to VEGF and cAMP. Flk1$^+$ cells were immunostained with anti-CD31 antibody (red) and anti-COUP-TFII antibody (green). Nuclei were stained with DAPI (blue). (**d**–**e**) Quantitative expression analysis of the venous marker genes *COUP-TFII* and *APJ* in the Flk1$^+$ cells (normalized to *GAPDH* mRNA; $n=3$). (**d**) The expression of *COUP-TFII* mRNA was increased exclusively by the combined treatment with VEGF, cAMP and COMP-Ang1. (**e**) The expression of *APJ* mRNA in the Flk1$^+$ cells was significantly upregulated by stimulation with VEGF and Ang1 compared with treatment with VEGF alone. *APJ* mRNA was further upregulated by the addition of COMP-Ang1 to VEGF and cAMP. The results were expressed as relative intensity over cells treated with VEGF. Scale bars, 50 μm. Values are shown as means ± s.e.m. for three separate experiments. One-way analysis of variance was used to compare differences. $^*P<0.05$, $^{**}P<0.01$, $^{***}P<0.001$ for the indicated groups.

formation as evaluated by either coronary arteriogram with ink injection or detection of EphrinB2-lacZ-positive coronary arteries (Fig. 3). Wu *et al.*[11] recently reported that both cardiomyocyte-specific VEGF-A KO mice and endocardium-specific VEGFR2 KO mice exhibit specific defects in coronary artery formation, but not in coronary vein formation. They reported that the ECs of the ventricular endocardium, but not those of the SV, generate the endothelium of coronary arteries. Their findings complement our findings obtained with Ang1CKO mice, suggesting that the formation of coronary arteries and veins might be distinctly regulated by VEGF-A/VEGFR2 signalling and Ang1/Tie2 signalling, respectively.

On the other hand, Red-Horse *et al.*[9] reported that the ECs of the SV are the common originators of both coronary arteries and veins, using clonal analysis, crossing *VE-Cadherin-Cre(ER)T2* mice with either *Rosa-lacZ* or multicolour *Cre* recombination reporters, and organ culture experiments combining the SV and atrium from *Apelin-nLacZ*-reporter mice with ventricles from wild-type mice. We also performed organ culture experiments combining the SV and atrium from *Tie2-lacZ* reporter mice with the ventricles and epicardium from either wild-type or Ang1CKO mice. These experiments suggested that Ang1 derived from the ventricular myocardium might attract the Tie2-positive ECs from the SV towards the ventricular myocardium presumably via promotion of migration and proliferation of the immature ECs (Fig. 5). Since we could not address the arterial–venous identity of the Tie2-positive ECs migrating into the wild-type ventricles due to the loss of the antigenicity in the organ culture samples, we cannot exclude the possibility that the ECs of SV might partly contribute to the formation of coronary arteries independent of the action of myocardial Ang1. So, the issues on the origin of the coronary arteries should be clarified in the future.

Katz *et al.*[10] recently reported that the Semaphorin3D/Scleraxis lineage-traced proepicardial cells, which migrate via SV endothelium into the myocardium and/or transiently contribute to the endocardium, differentiate into the coronary ECs. This finding indicates that the proepicardial cells as well as the SV ECs might be one candidate source for coronary vein ECs. Since there have been no appropriate reporter mice to specifically trace the lineage of the SV ECs to date, we should determine the origins of the coronary veins through identifying the marker genes specifically expressed in the ECs of the SV in the future.

Ang1 is reported to enhance the migration of the vascular ECs in cooperation with VEGF[33]. Consistent with this finding, Ang1CKO mice showed impaired migration of subepicardial immature APJ-negative ECs compared with control mice (Fig. 1 and Supplementary Fig. 2). Since the coronary artery formation was almost intact in Ang1CKO mice (Fig. 3), the myocardium-derived VEGF-dependent signalling and migration of ECs appeared to be preserved in these mice. These data indicate that Ang1 might regulate the migration of immature ECs from the SV into the myocardium in cooperation with VEGF derived from the myocardium.

On the other hand, we also found that Ang1CKO embryos showed impaired proliferation of subepicardial ECs compared with control embryos (Supplementary Fig. 9a–c). Previous studies revealed that Ang1 exerts opposing effects such as proliferation and stabilization of the cell–cell contact of the ECs depending on

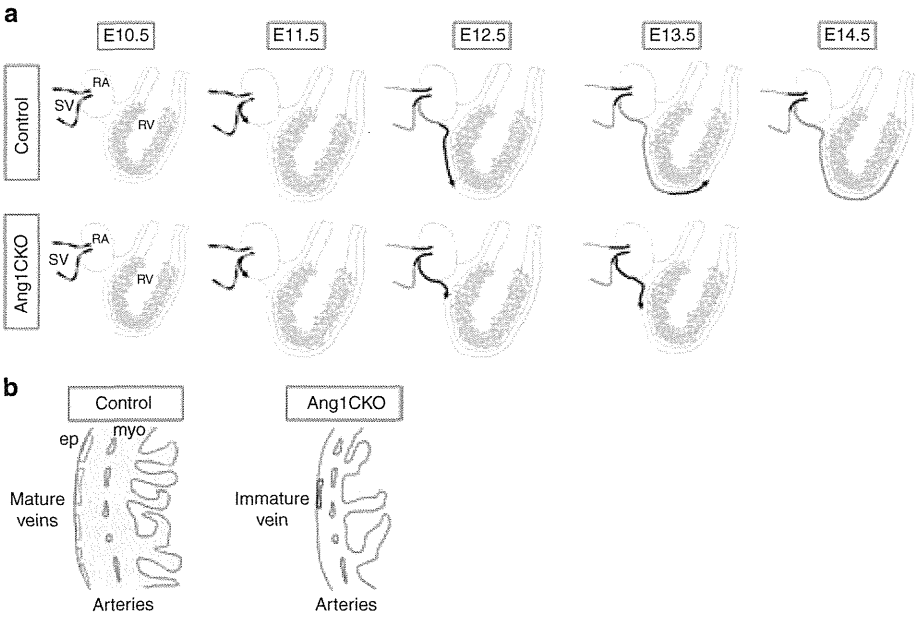

Figure 9 | Role of Ang1 on coronary vessel formation. (**a**) Working model of coronary vein formation. The upper panel shows a schematic illustration of coronary vein formation in wild-type mice. The ECs in the SV at E10.5 consist of APJ-positive mature ECs (blue) and APJ-negative immature ECs (black). The APJ-negative ECs sprout off from the SV into the RA at E11.5. While the APJ-negative ECs migrate from the RA into the RV at E12.5, the APJ-negative ECs in the RA undergo venous differentiation in response to the action of Ang1 secreted from the myocardium, and differentiate into APJ-positive mature venous ECs. At E13.5, the APJ-negative ECs continue to migrate ahead of the APJ-positive ECs, which have emerged on the surface of the RV. At E14.5, all of the subepicardial CD31-positive cells have differentiated into mature venous APJ-positive ECs. In Ang1CKO mice, the migration, the proliferation and the venous specification of the APJ-negative ECs are impaired, resulting in defective coronary vein formation (lower panels). (**b**) Schematic diagram of coronary vessel formation in Ang1CKO embryo. Cardiomyocyte-specific deletion of Ang1 disturbs coronary vein formation, but does not impair coronary artery formation. Blue: APJ-positive ECs, Black: APJ-negative ECs. ep, epicardium; myo, myocardium; RA, right atrium; RV, right ventricle; SV, sinus venosus.

the cellular contexts[34,35]. While Angl can bridge Tie2 at cell–cell contacts and mediates *trans*-association of Tie2 in the presence of cell–cell contacts, extracellular matrix-bound Angl locates Tie2 at cell–substratum contacts in isolated cells[34]. Of note, Tie2 activated at cell–cell or cell–substratum contacts leads to preferential activation of Akt and Erk, respectively[34,35], suggesting that Angl can evoke distinct cellular responses in the ECs according to the cellular environment. Taken together, myocardial Angl might contribute to the formation of coronary veins by promoting both proliferation and migration of the immature ECs derived from SV.

The ECs of the SV were found to be heterogeneous, consisting of both APJ-positive and -negative cells. Among the ECs in the SV, only the APJ-negative ECs were found to migrate into the atrium and ventricles. Furthermore, all of the atrial subepicardial ECs were APJ-positive following 1 day of exposure to Angl expressed in the atrial myocardium (Fig. 6). Thus, the APJ-positive ECs appeared to be produced through differentiation of the APJ-negative ECs by the action of myocardial Angl.

Our findings indicate that myocardial Angl has a critical role in coronary vein formation by mediating the migration, proliferation and venous differentiation of immature ECs in the developing hearts. Elucidation of the molecular mechanisms underlying Angl-mediated venous differentiation will provide insight into heart disease and tissue regeneration.

Methods

Animals. The targeting vector for creating $Angl^{flox}$ allele was constructed by inserting *loxP/PGK-Neo-pA/loxP* into exon 1 of the genomic *Angl* locus[17]. The targeting vector was introduced into TT2 embryonic stem cells. The targeted embryonic stem cell clones were injected into CD-1 8-cell stage embryos, and the resultant male chimera mice were mated with C57BL/6 females to establish germ line transmission. $Angl^{flox(neo+)}$ mice were maintained in CBA/C57BL/6/CD-1 mixed background. The neomycin cassette in $Angl^{flox(neo+)}$ allele was excised through crossing with *CAG-FLPe* transgenic mice in C57BL/6 background (B6-Tg(*CAG-FLPe*)36)[36]. To create Ang1CKO mice, we crossed $Angl^{flox/flox}$ mice with α-*MHC-Cre* transgenic mice in a C57BL/6 background[16,17]. *Tie2-lacZ* transgenic (FVB/N-Tg(*TIE2-lacZ*)182Sato/J) mice were purchased from the Jackson Laboratory[30]. The *EphB4 tau-lacZ* knockin mice and *EphrinB2 tau-lacZ* knockin mice were used for determination of the arterial–venous lineages of the coronary ECs[23,27]. Enhanced green fluorescent protein (EGFP) reporter mice (CAG-CAT-EGFP) were obtained from J. Miyazaki, Osaka University[37]. The *Angl-mCherry* gene construct was generated from a BAC clone (RP23-5J11) containing a 144-kb genomic fragment spanning the region upstream of the *Angl* locus. The targeting vector used to modify BAC RP23-5J11 was designed to insert the *mCherry* sequence into the first coding exon of the *Angl* gene. The 5′ and 3′ homology sequence, the *mCherry* gene, and the fragment including the poly A sequence were cloned into PL453, which contained the neomycin-resistance cassette flanked by Frt sites.

All animals were maintained in a virus-free facility on a 12-h light/12-h dark cycle and fed a standard mouse diet. All experiments were carried out under the guidelines of the Osaka University Committee for animal and recombinant DNA experiments and were approved by the Osaka University Institutional Review Board.

Genotyping of the animals. The PCR primers used for genotyping were as follows: Angl flox: 5′-CCGGATTCAACATGGGCAATGTGCC-3′, 5′-CAGTCA AAATGCCTAAGATAAAC-3′; Cre: 5′-ACATGTTCAGGGATCGCCAG-3′, 5′-TAACCAGTGAAACAGCATTGC-3′; lacZ: 5′-CAGACGATGGTGCAGGAT AT-3′, 5′-ATACAGCGCGTCGTGATTAG-3′; Angl-mCherry: 5′-AGGACGGCG AGTTCATCTAC-3′, 5′-TGGTGTAGTCCTCGTTGTGG-3′; EGFP: 5′-AGCAA GGGCGAGGAGCTGTT-3′, 5′-GTAGGTCAGGGTGGTCACGA-3′.

Detection of β-galactosidase activity in embryonic tissues. Embryonic tissues were fixed in 0.2% glutaraldehyde in phosphate-buffered saline (PBS) containing 5 mM EGTA and 2 mM $MgCl_2$ at 4 °C for 4 h, washed in washing buffer (2 mM $MgCl_2$, 0.02% NP-40, 0.1% sodium deoxycholate in PBS) for 30 min three times,

cryoprotected with 30% sucrose, and frozen in OCT compound (Tissue Tek) and cryosectioned. Samples were stained in X-gal staining buffer (5 mM potassium ferricyanide, 5 mM potassium ferrocyanide, 1 mg/ml X-gal in washing buffer) at 37 °C.

Histological analysis. Dissected embryonic hearts were fixed in 4% paraformaldehyde (PFA)/PBS overnight at 4 °C, embedded in paraffin and sectioned at 7 μm thickness. Hematoxylin/eosin staining was performed according to standard procedures on the paraffin sections[16].

Immunohistochemical analysis. The following antibodies were used: anti-CD31 (550274) and anti-VEGFR2 (550549) (BD Pharmingen), anti-Tie2 (sc-324, Santa Cruz), anti-beta-galactosidase (NB100-2045, Novus Biologicals), anti-DsRed (632496, Clontech), anti-phospho-Histone H3 (Ser10) (06-570, Merck Millipore). The whole-mount immunohistochemistry of mouse embryos using anti-CD31 monoclonal (1:100) and anti-APJ antibodies (1:100) was performed[38,39]. Embryonic hearts were dissected and fixed in 4% PFA/PBS overnight at 4 °C. Samples were washed in PBS, dehydrated in absolute methanol (MeOH) and stored at −20 °C until antibody staining. Embryonic hearts were incubated in Dent's bleach (MeOH: dimethyl sulfoxide: 30%H_2O_2, 4:1:1) for 3 h at room temperature and washed with a series of descending MeOH/PBST (PBS + 0.1% Triton-X) concentrations (70%MeOH, 50%MeOH, PBST). Samples were blocked in 2% skimmed milk for 1 h and incubated with primary antibodies overnight at 4 °C. Next day samples were washed three times for 1 h with PBST and incubated with secondary antibodies overnight at 4 °C. Finally samples were washed three times for 1 h with PBST and applied with DAB (Invitrogen) at room temperature. When necessary, 7 μm sections were cut from paraffin-embedded whole-mounts.

For frozen section immunohistochemistry, embryos or isolated embryonic hearts were fixed for 4 h to overnight in 4% PFA/PBS. Fixed embryos or hearts were soaked in a 15–30% sucrose gradient before being embedded in OCT (Tissue Tek) for frozen sections and cut by cryosectioning (10 μm). Sections were rehydrated in PBS, incubated in blocking solution containing either 5% normal goat serum, 1% bovine serum albumin and 2% skim milk or 10% normal goat serum in PBST for 1 h and then incubated with primary antibodies (CD31 1:300, Tie2 1:200, APJ 1:300, VEGFR2 1:100, Beta-galactosidase 1:4000, DsRed 1:1000, phospho Historne H3 1:100) in Can Get Signal immunostain (TOYOBO, NKB-601) overnight at 4 °C. Sections were then washed in PBST and incubated with fluorescent-conjugated (Invitrogen; Alexa Fluor 488 and 546) or horseradish peroxidase (HRP)-coupled (Cell Signaling Technology (7074), 1:200) secondary antibodies for 30 min to 1 h at room temperature. Images were acquired with a microscope (Keyence, BZ-9000).

Whole-mount *in situ* hybridization. Embryos were fixed in 4% PFA/PBS overnight at 4 °C and stored in 100% MeOH at −20 °C until hybridization. The Ang1 antisense probe was generated from mouse *Ang1* cDNA[18]. Whole-mount *in situ* hybridization was performed at 70 °C for 18 h for each sample[40]. The detection was performed with alkaline phosphatase-coupled anti-digoxygenin antibody (Boehringer Ingerheim) overnight at 4 °C. After washing, the chromogenic reaction was performed with NBT–BCIP substrate (Promega). Photographs were captured with a stereomicroscope (Olympus, SZX12).

***In situ* hybridization on frozen sections.** Embryos were fixed overnight in 4% PFA/PBS. Fixed embryos were soaked in a 15–30% sucrose gradient before being embedded in OCT (Tissue Tek) for frozen sections (10 μm). Sections were rehydrated in PBS. A 994 bp long *in situ* probe was generated of the mouse *COUP-TFII* gene (Forward: CGGAATTCTCAACTGCCACTCGTACCT, Reverse: CCACTAGTGCTTTCCACATGGGCTACAT). *In situ* hybridization was performed in a similar method to whole-mount *in situ* hybridization[40]. Hybridized DIG-RNA probes were detected with alkaline phosphatase-coupled anti-digoxygenin antibody overnight at 4 °C. Photographs were captured with BZ-9000 (KEYENCE).

Coronary arteriogram of murine embryos. Hearts were resected from embryos and placed in heparinized PBS. Ink (Kiwa-guro; Sailor) was injected in a retrograde fashion from the ascending aorta using a glass micropipette and fixed in 4% PFA/PBS[26]. Photographs were captured using a stereomicroscope (Olympus, SZX12).

Quantitative real-time RT-PCR. Quantitative real-time RT–PCR was carried out using the QuantiFast SYBRGreen RT–PCR kit (Qiagen)[39]. For each reaction, 80 ng of total RNA was transcribed for 10 min at 50 °C followed by a denaturing step at 95 °C for 5 min and 40 cycles of 10 s at 95 °C and 30 s at 60 °C. Fluorescence data were collected and analysed using ABI PRISM 7900HT. The primers used for amplification of total RNA from murine hearts were as follows: *GAPDH*: 5′-TCTCCACACCTATGGTGCAA-3′, 5′-CAAGAAACAGGGGAGCTGAG-3′; *Ang1* 5′-GCAGCCATAGCAATGCCAGAGGT-3′, 5′-TCCCATGGCAACTCACAAAACTCC-3′; *Efnb2*: 5′-TGTTGGGGACTTTTGATGGT-3′; 5′-GTCCACTTTGGGGCAAATAA-3′; *Ephb4*: 5′-CTGGATGGAGAACCCCTACA-3′, 5′-CCAGGTAGAAGCCAGCTTTG-3′; *COUP-TFII*: 5′-GCAAGTGGAGAAGCTCAAGG-3′, 5′-TTCCAAAGCACACTGGGACT-3′; *Notch1*: 5′-TGTTGTGCTCCTGAAGAACG-3′, 5′-TCCATGTGATCCGTGATGTC-3′; *Dll4*: 5′-TGCCTGGGAAGTATCCTCAC-3′, 5′-GTGGCAATCACACACTCGTT-3′; *Acvrl1*: 5′-CCAATGACCCCAGTTTTGAG-3′, 5′-TTGGGGTACCAGCACTCTCT-3′; *Hes1*: 5′-ATCATGGAGAAGAGGCGAAG-3′, 5′-CGGAGGTGCTTCACAGTCAT-3′; *Nrp1*: 5′-CCGGAACCCTACCAGAGAAT-3′, 5′-AAGGTGCAATCTTCCCACAG-3′; *APJ*: 5′-CAGTCTGAATGCGACTACGC-3′, 5′-CCATGACAGGCACAGCTAGA-3′.

Organ cultures. Heart cultures were carried out according to the previous report[9]. In brief, embryonic hearts were dissected from wild-type, *Tie2-lacZ* or Ang1CKO embryos, and the atria and attached sinus venosus (SV/A) were then dissected from the ventricles. The SV/A tissues from the *Tie2-lacZ* embryos were placed adjacent to the ventricles of either wild-type or Ang1CKO embryos at the position where the original SV/A was removed. The explants were cultured dorsal side up at the air–liquid interface on 8-mm Millicell Cell Culture Insert Filters (Merck Millipore). Cultures were maintained at 37 °C and 5% CO_2 in DMEM with 2 μg ml^{-1} heparin, 100 U ml^{-1} penicillin, 100 μg ml^{-1} streptomycin, 2 mM L-glutamine and 10% fetal bovine serum. After 72 h, explants were fixed with 4% PFA/PBS and subjected to whole-mount X-gal staining. Some stained explants were embedded in paraffin and then sectioned.

Cell culture and differentiation of embryonic stem cells. ES cell lines EStTA-ROSA, and various EStTA derivatives were maintained with Glasgow's MEM (GMEM; Invitrogen) containing 1×10^{-4} M 2-mercaptoethanol (Invitrogen), 10% knockout serum replacement (KSR; Invitrogen), 1% fetal calf serum (FCS; SAFC Biosciences), 1 mM sodium pyruvate (Sigma), 1% non-essential amino acids solution (Invitrogen) and 2×10^3 U ml^{-1} leukaemia inhibitory factor (Merck Millipore). Differentiation was induced in these ES cell lines using differentiation medium (DM) consisting of minimum essential medium alpha (Invitrogen) supplemented with 10% FCS (Invitrogen) and 5×10^{-5} M 2-mercaptoethanol[31,41]. In brief, undifferentiated ES cells were cultured on gelatin-coated dishes without leukaemia inhibitory factor at a density of 0.75–10^3 cells per cm^2 for 4.5 days. Cultured cells were harvested and subjected to magnetic cell sorting (MACS) purification. Purified Flk1$^+$ cells were then plated onto gelatin-coated dishes at a density of 0.75–10^4 cells per cm^2 in DM. After 3 days, induced ECs were examined by immunocytochemistry and FACS analysis. Human $VEGF_{165}$ (WAKO, 50 μg ml^{-1}) and 8-bromoadenosine-3′, 5′-cyclic monophosphate sodium salt (8-bromo-cAMP; Nacalai, 0.5 mM) were added to the Flk1$^+$ cell culture. COMP-Ang1 was added to the Flk1$^+$ cell culture at the concentration of 100 ng ml^{-1} (ref. 32).

Stealth siRNAs targeting murine *Tie2* gene were purchased from Invitrogen (MSS211290, MSS211291, MSS278161). Cells were transfected with mixed three siRNAs (total 50 nM) 12 h before Flk1$^+$ cell purification using Lipofectamine RNAiMAX reagent (Invitrogen) according to the manufacturer's instructions. Furthermore, Flk1$^+$ cells were plated and simultaneously transfected with mixed siRNAs (total 20 nM).

Immunocytochemical analysis of Flk1$^+$ cells. The cultured ECs were immunostained according to the previous report[41]. Briefly, for double-fluorescence staining of COUP-TFII and CD31, ECs were fixed with 4% PFA/PBS. Fixed culture slides were incubated with anti-COUP-TFII antibody (H7147, Perseus Proteomics) and anti-CD31 (550274, BD Pharmingen). Culture slides were then washed in PBST and incubated with fluorescent-conjugated secondary antibodies (Invitrogen; Alexa Fluor 488 and 546). For double-fluorescence staining of EphrinB2 and CD31, ECs were fixed with 5% dimethyl sulfoxide/MeOH. Fixed culture slides were incubated with EphB4-human immunoglobulin (Ig) Fc portion chimeric protein (EphB4-Fc; R&D Systems) followed by human IgG Fc peroxidase-conjugated goat IgG fraction (ICN Biomedicals). The TSA biotin system (PerkinElmer) was used to amplify the signal for EphB4-Fc staining. EphrinB2-positive cells were visualized with streptavidin/Alexa Fluor 488 conjugate (Invitrogen). CD31-positive cells were stained with PE-conjugated mAb for CD31.

Statistical analysis. All data were expressed as means ± s.e.m. Differences among multiple groups were compared by one-way analysis of variance. Student's *t*-test was used to analyse differences between two groups. A value of $P < 0.05$ was considered as statistically significant.

References

1. Luttun, A. & Carmeliet, P. De novo vasculogenesis in the heart. *Cardiovasc. Res.* **58,** 378–389 (2003).
2. Riley, P. R. & Smart, N. Vascularizing the heart. *Cardiovasc. Res.* **91,** 260–268 (2011).
3. Del Monte, G. & Harvey, R. P. An endothelial contribution to coronary vessels. *Cell* **151,** 932–934 (2012).
4. Guadix, J. A., Carmona, R., Munoz-Chapuli, R. & Perez-Pomares, J. M. In vivo and in vitro analysis of the vasculogenic potential of avian proepicardial and epicardial cells. *Dev. Dyn.* **235,** 1014–1026 (2006).

5. Mikawa, T. & Fischman, D. A. Retroviral analysis of cardiac morphogenesis: discontinuous formation of coronary vessels. *Proc. Natl Acad. Sci. USA* **89,** 9504–9508 (1992).
6. Perez-Pomares, J. M. *et al.* Origin of coronary endothelial cells from epicardial mesothelium in avian embryos. *Int. J. Dev. Biol.* **46,** 1005–1013 (2002).
7. Cai, C. L. *et al.* A myocardial lineage derives from Tbx18 epicardial cells. *Nature* **454,** 104–108 (2008).
8. Zhou, B. *et al.* Epicardial progenitors contribute to the cardiomyocyte lineage in the developing heart. *Nature* **454,** 109–113 (2008).
9. Red-Horse, K., Ueno, H., Weissman, I. L. & Krasnow, M. A. Coronary arteries form by developmental reprogramming of venous cells. *Nature* **464,** 549–553 (2010).
10. Katz, T. C. *et al.* Distinct compartments of the proepicardial organ give rise to coronary vascular endothelial cells. *Dev. Cell* **22,** 639–650 (2012).
11. Wu, B. *et al.* Endocardial cells form the coronary arteries by angiogenesis through myocardial-endocardial VEGF signaling. *Cell* **151,** 1083–1096 (2012).
12. Augustin, H. G., Koh, G. Y., Thurston, G. & Alitalo, K. Control of vascular morphogenesis and homeostasis through the angiopoietin-Tie system. *Nat. Rev. Mol. Cell. Biol.* **10,** 165–177 (2009).
13. Davis, S. *et al.* Isolation of angiopoietin-1, a ligand for the TIE2 receptor, by secretion-trap expression cloning. *Cell* **87,** 1161–1169 (1996).
14. Sato, T. N. *et al.* Distinct roles of the receptor tyrosine kinases Tie-1 and Tie-2 in blood-vessel formation. *Nature* **376,** 70–74 (1995).
15. Suri, C. *et al.* Requisite role of angiopoietin-1, a ligand for the TIE2 receptor, during embryonic angiogenesis. *Cell* **87,** 1171–1180 (1996).
16. Nakaoka, Y. *et al.* Gab family proteins are essential for postnatal maintenance of cardiac function via neuregulin-1/ErbB signaling. *J. Clin. Invest.* **117,** 1771–1781 (2007).
17. Lee, J. *et al.* Angiopoietin-1 guides directional angiogenesis through integrin alphavbeta5 signaling for recovery of ischemic retinopathy. *Sci. Transl. Med.* **5,** 203ra127 (2013).
18. Nagase, T., Nagase, M., Yoshimura, K., Fujita, T. & Koshima, I. Angiogenesis within the developing mouse neural tube is dependent on sonic hedgehog signaling: possible roles of motor neurons. *Genes Cells* **10,** 595–604 (2005).
19. Jeansson, M. *et al.* Angiopoietin-1 is essential in mouse vasculature during development and in response to injury. *J. Clin. Invest.* **121,** 2278–2289 (2011).
20. Lavine, K. J., Long, F. X., Choi, K., Smith, C. & Ornitz, D. M. Hedgehog signaling to distinct cell types differentially regulates coronary artery and vein development. *Development* **135,** 3161–3171 (2008).
21. Claxton, S. & Fruttiger, M. Oxygen modifies artery differentiation and network morphogenesis in the retinal vasculature. *Dev. Dyn.* **233,** 822–828 (2005).
22. Saint-Geniez, M., Argence, B., Knibiehler, B. & Audigier, Y. The msr/apj gene encoding the apelin receptor is an early and specific marker of the venous phenotype in the retinal vasculature. *Gene Expr. Patterns* **3,** 467–472 (2003).
23. Gerety, S. S., Wang, H. U., Chen, Z. F. & Anderson, D. J. Symmetrical mutant phenotypes of the receptor EphB4 and its specific transmembrane ligand ephrin-B2 in cardiovascular development. *Mol. Cell* **4,** 403–414 (1999).
24. Pereira, F. A., Qiu, Y., Zhou, G., Tsai, M. J. & Tsai, S. Y. The orphan nuclear receptor COUP-TFII is required for angiogenesis and heart development. *Genes Dev.* **13,** 1037–1049 (1999).
25. You, L. R. *et al.* Suppression of Notch signalling by the COUP-TFII transcription factor regulates vein identity. *Nature* **435,** 98–104 (2005).
26. Arima, Y. *et al.* Preotic neural crest cells contribute to coronary artery smooth muscle involving endothelin signalling. *Nat. Commun.* **3,** 1267 (2012).
27. Wang, H. U., Chen, Z. F. & Anderson, D. J. Molecular distinction and angiogenic interaction between embryonic arteries and veins revealed by ephrin-B2 and its receptor Eph-B4. *Cell* **93,** 741–753 (1998).
28. Yamamizu, K. & Yamashita, J. K. Roles of cyclic adenosine monophosphate signaling in endothelial cell differentiation and arterial-venous specification during vascular development. *Circ. J.* **75,** 253–260 (2011).
29. Garratt, A. N., Ozcelik, C. & Birchmeier, C. ErbB2 pathways in heart and neural diseases. *Trends Cardiovasc. Med.* **13,** 80–86 (2003).
30. Schlaeger, T. M. *et al.* Uniform vascular-endothelial-cell-specific gene expression in both embryonic and adult transgenic mice. *Proc. Natl Acad. Sci. USA* **94,** 3058–3063 (1997).
31. Yamashita, J. *et al.* Flk1-positive cells derived from embryonic stem cells serve as vascular progenitors. *Nature* **408,** 92–96 (2000).
32. Cho, C. H. *et al.* COMP-Ang1: a designed angiopoietin-1 variant with nonleaky angiogenic activity. *Proc. Natl Acad. Sci. USA* **101,** 5547–5552 (2004).
33. Chae, J. K. *et al.* Coadministration of angiopoietin-1 and vascular endothelial growth factor enhances collateral vascularization. *Arterioscler. Thromb. Vasc. Biol.* **20,** 2573–2578 (2000).
34. Fukuhara, S. *et al.* Differential function of Tie2 at cell-cell contacts and cell-substratum contacts regulated by angiopoietin-1. *Nat. Cell Biol.* **10,** 513–526 (2008).
35. Saharinen, P. *et al.* Angiopoietins assemble distinct Tie2 signalling complexes in endothelial cell-cell and cell-matrix contacts. *Nat. Cell Biol.* **10,** 527–537 (2008).
36. Kanki, H., Suzuki, H. & Itohara, S. High-efficiency CAG-FLPe deleter mice in C57BL/6J background. *Exp. Anim.* **55,** 137–141 (2006).
37. Kawamoto, S. *et al.* Suppression of T(h)1 cell activation and prevention of autoimmune diabetes in NOD mice by local expression of viral IL-10. *Int. Immunol.* **13,** 685–694 (2001).
38. Kidoya, H. *et al.* Spatial and temporal role of the apelin/APJ system in the caliber size regulation of blood vessels during angiogenesis. *EMBO J.* **27,** 522–534 (2008).
39. Shioyama, W. *et al.* Docking protein Gab1 is an essential component of postnatal angiogenesis after ischemia via HGF/c-met signaling. *Circ. Res.* **108,** 664–675 (2011).
40. Shirai, M., Imanaka-Yoshida, K., Schneider, M. D., Schwartz, R. J. & Morisaki, T. T-box 2, a mediator of Bmp-Smad signaling, induced hyaluronan synthase 2 and Tgfbeta2 expression and endocardial cushion formation. *Proc. Natl Acad. Sci. USA* **106,** 18604–18609 (2009).
41. Yamamizu, K. *et al.* Convergence of Notch and beta-catenin signaling induces arterial fate in vascular progenitors. *J. Cell Biol.* **189,** 325–338 (2010).

Acknowledgements

We thank Yuka Yoshimoto for secretarial assistance; Miki Nagase (Tokyo University) for providing the plasmid containing the mouse Ang1 in situ hybridization probe; David J. Anderson (California Institute of Technology) for providing the *EphB4 tau-lacZ* and *EphrinB2 tau-lacZ* knock-in mice; and Satoshi Somekawa (Nara Medical University) for helpful comments. This work was supported in part by grants from the Ministry of Education, Science, Sports and Culture of Japan (to I.K., Y.N.); Japan Heart Foundation Young Investigator's Research Grant (to Y.N.); Suzuken Memorial Foundation (to Y.N.); Astellas Foundation for Research on Metabolic Disorders (to Y.N.); Senri Life Science Foundation (to Y.N.); Miyata Cardiology Research Promotion Funds (to Y.N.); Mochida Memorial Foundation for Medical and Pharmaceutical Research (to Y.N.); Takeda Medical Research Foundation (to Y.N.); Daiichi-Sankyo Foundation of Life Science (to Y.N.); SENSHIN Medical Research Foundation (to Y.N.); Kobayashi Magobe (Mannari Hospital) Medical Research Foundation (to Y.N.); Japan Heart Foundation/Novartis Grant for Research Award on Molecular and Cellular Cardiology, 2012 (to Y.A.).

Author contributions

Yo.A. performed most of experiments in mice, analysed data, wrote manuscripts; Y.N. designed this study, wrote manuscript, created mice through crossing, analysed data and supervised this study; T.Mat., K.Y., and J.K.Y. performed experiments using Flk1 + vascular progenitor cells and analysed data; Yu.A., K.N. and H.Ku. performed the experiments of murine coronary arteriogram; H.Ki., T.K.-H., K.I., T.Y., T.Mas., K.Y., K.H., M.S., H.Y. and T.Mi. performed the mice experiment; K.O., N.M. and N.T. contributed to the generation of mice; K.Y.-T., and Y.S. helped the design of this study; J.-S.P. and G.Y.K. generated COMP-angiopoietin-1; I.K. edited the manuscript and supervised this project generally.

Additional information

Supplementary Information accompanies this paper at http://www.nature.com/naturecommunications

Competing financial interests: The authors declare no competing financial interests.

Reprints and permission information is available online at http://npg.nature.com/reprintsandpermissions/

How to cite this article: Arita, Y. *et al.* Myocardium-derived angiopoietin-1 is essential for coronary vein formation in the developing heart. *Nat. Commun.* 5:4552 doi: 10.1038/ncomms5552 (2014).

Diabetologia (2014) 57:1968–1976
DOI 10.1007/s00125-014-3306-9

ARTICLE

Selenoprotein P as a diabetes-associated hepatokine that impairs angiogenesis by inducing VEGF resistance in vascular endothelial cells

Kazuhide Ishikura · Hirofumi Misu · Masafumi Kumazaki · Hiroaki Takayama · Naoto Matsuzawa-Nagata · Natsumi Tajima · Keita Chikamoto · Fei Lan · Hitoshi Ando · Tsuguhito Ota · Masaru Sakurai · Yumie Takeshita · Kenichiro Kato · Akio Fujimura · Ken-ichi Miyamoto · Yoshiro Saito · Satomi Kameo · Yasuo Okamoto · Yoh Takuwa · Kazuhiko Takahashi · Hiroyasu Kidoya · Nobuyuki Takakura · Shuichi Kaneko · Toshinari Takamura

Received: 10 January 2014 / Accepted: 30 May 2014 / Published online: 3 July 2014

Abstract

Aims/hypothesis Impaired angiogenesis induced by vascular endothelial growth factor (VEGF) resistance is a hallmark of vascular complications in type 2 diabetes; however, its molecular mechanism is not fully understood. We have previously identified selenoprotein P (SeP, encoded by the *SEPP1* gene in humans) as a liver-derived secretory protein that induces insulin resistance. Levels of serum SeP and hepatic expression of *SEPP1* are elevated in type 2 diabetes. Here, we investigated the effects of SeP on VEGF signalling and angiogenesis.

Methods We assessed the action of glucose on *Sepp1* expression in cultured hepatocytes. We examined the actions of SeP on VEGF signalling and VEGF-induced angiogenesis in HUVECs. We assessed wound healing in mice with hepatic SeP overexpression or SeP deletion. The blood flow recovery after ischaemia was also examined by using hindlimb ischaemia model with *Sepp1*-heterozygous-knockout mice.

Kazuhide Ishikura, Hirofumi Misu and Masafumi Kumazaki contributed equally to this work.

Electronic supplementary material The online version of this article (doi:10.1007/s00125-014-3306-9) contains peer-reviewed but unedited supplementary material, which is available to authorised users.

K. Ishikura · H. Misu · M. Kumazaki · H. Takayama · N. Matsuzawa-Nagata · N. Tajima · K. Chikamoto · F. Lan · H. Ando · T. Ota · M. Sakurai · Y. Takeshita · K. Kato · S. Kaneko · T. Takamura (✉)
Department of Disease Control and Homeostasis, Kanazawa University Graduate School of Medical Sciences, 13-1 Takara-machi, Kanazawa, Ishikawa 920-8641, Japan
e-mail: ttakamura@m-kanazawa.jp

M. Kumazaki · H. Ando · A. Fujimura
Division of Clinical Pharmacology, Department of Pharmacology, Jichi Medical University, Tochigi, Japan

N. Matsuzawa-Nagata · K. Miyamoto
Department of Medicinal Informatics, Kanazawa University Graduate School of Medical Sciences, Kanazawa, Ishikawa, Japan

M. Sakurai
Department of Epidemiology and Public Health, Kanazawa Medical University, Uchinada, Japan

Y. Saito
Department of Medical Life Systems, Faculty of Medical and Life Sciences, Doshisha University, Kyotanabe, Kyoto, Japan

S. Kameo
Department of Public Health, Gunma University Graduate School of Medicine, Gunma, Japan

Y. Okamoto · Y. Takuwa
Department of Physiology, Kanazawa University Graduate School of Medical Sciences, Kanazawa, Ishikawa, Japan

K. Takahashi
Department of Nutritional Biochemistry, Hokkaido Pharmaceutical University, Otaru, Hokkaido, Japan

H. Kidoya · N. Takakura
Department of Signal Transduction, Research Institute for Microbial Diseases, Osaka University, Osaka, Japan

Results Treatment with glucose increased gene expression and transcriptional activity for *Sepp1* in H4IIEC hepatocytes. Physiological concentrations of SeP inhibited VEGF-stimulated cell proliferation, tubule formation and migration in HUVECs. SeP suppressed VEGF-induced reactive oxygen species (ROS) generation and phosphorylation of VEGF receptor 2 (VEGFR2) and extracellular signal-regulated kinase 1/2 (ERK1/2) in HUVECs. Wound closure was impaired in the mice overexpressing *Sepp1*, whereas it was improved in $SeP^{-/-}$mice. $SeP^{+/-}$mice showed an increase in blood flow recovery and vascular endothelial cells after hindlimb ischaemia.

Conclusions/interpretation The hepatokine SeP may be a novel therapeutic target for impaired angiogenesis in type 2 diabetes.

Keywords Angiogenesis · Hepatokine · ROS · Selenoprotein P · VEGF

Abbreviations

BSO	Buthionine sulfoximine
DCF	2′,7′-Dichlorofluorescein diacetate
ERK1/2	Extracellular signal-regulated kinase 1/2
MAPK	Mitogen-activated protein kinase
ROS	Reactive oxygen species
SeP	Selenoprotein P
VEGF(R)	Vascular endothelial growth factor (receptor)

Introduction

Type 2 diabetes is a chronic hyperglycaemic condition that causes various vascular complications, including damage to: small blood vessels, resulting in retinopathy, nephropathy and neuropathy; and large blood vessels, resulting in cardiovascular diseases. Earlier improved glycaemic control is associated with reduced risk for cardiovascular disease in people with type 2 diabetes [1]. However, more recent clinical trials have indicated that strict glycaemic control does not necessarily prevent vascular complications [2]. Hence, beyond glycaemic control, novel therapies to directly treat vascular disease are needed to improve the prognosis of people with type 2 diabetes.

Angiogenesis is a physiological process involving the growth of new blood vessels from pre-existing vascular structures and the subsequent formation of a vascular network. A number of abnormalities associated with angiogenesis have been observed in people with type 2 diabetes [3], and impaired angiogenesis is linked to the development of various vascular complications in diabetes mellitus. Compared with control individuals without diabetes, people with type 2 diabetes show poor development of coronary collateral vessels on coronary angiography [4]. Moreover, a previous study using autopsied hearts reported that people with diabetes have significantly lower capillary densities in areas of myocardial infarction [5]. These reports suggest that the angiogenic response to infarction and/or ischaemia is inhibited at the levels of capillaries and small arterioles in type 2 diabetes. Inadequate vascular formation could attenuate perfusion recovery in response to ischaemia, thereby partially accounting for the poor clinical outcomes in type 2 diabetic patients with coronary heart disease or peripheral artery disease [6, 7]. In addition, insufficient angiogenesis is involved in abnormal wound healing and the development of diabetic skin ulcers [8].

Vascular endothelial growth factor (VEGF) is a major mediator of angiogenesis under physiological and pathophysiological conditions. VEGF binds and phosphorylates its receptors, leading to the activation of a variety of signalling cascades such as the mitogen-activated protein kinase (MAPK) and Akt cascades. Angiogenic gene therapy using plasmids encoding VEGF has been attempted in patients with coronary or peripheral artery diseases [9]. However, diabetes mellitus people often show a poor response to therapeutic angiogenesis [10]. Therefore, VEGF resistance, a defect of VEGF-related signal transduction, has been postulated as a molecular basis for the dysregulated angiogenesis in diabetes mellitus [3, 11]. The molecular mechanisms underlying VEGF resistance in diabetes mellitus are not fully understood.

Selenoprotein P (SeP, encoded by *SEPP1* in humans and *Sepp1* in mice) is a secretory protein produced primarily in the liver [12, 13]. It contains ten selenocysteine residues and functions as a selenium supply protein [14]. We have previously reported that levels of serum SeP and hepatic gene expression of *SEPP1* are elevated in type 2 diabetes [15]. More recently, Yang et al have reported that serum levels of SeP are increased in people with impaired glucose tolerance [16]. SeP impairs insulin signal transduction and induces dysregulation of glucose metabolism in skeletal muscle and liver, indicating that SeP functions as a type 2 diabetes-associated hepatokine that causes insulin resistance and hyperglycaemia [15]. SeP has heparin-binding properties [17] and is associated with endothelial cells in rat tissues [18], suggesting that SeP exerts some actions on vascular endothelial cells. A previous study using in vitro techniques reported that SeP has an antioxidative action in vascular endothelial cells [19]. Nevertheless, it is unknown whether SeP plays a role in the angiogenic response.

We speculated that the liver-derived secretory protein SeP contributes to angiogenesis-associated vascular complications in type 2 diabetes by acting directly on vascular endothelial cells. In the current study, we investigated the effects of SeP on angiogenesis in normal conditions, independently of diabetes, using purified SeP protein and *Sepp1*-deficient mice without the induction of diabetes.

Methods

Cell culture HUVECs were cultured in HuMedia EG2 (Kurabo, Osaka, Japan). H4-II-E-C3 cells were cultured in 10% (vol./vol.) fetal bovine serum (FBS)/DMEM (Gibco, Carlsbad, CA, USA) as previously described [20]. All cellular experiments were approved by the Committee for Cellular Study at our Institute.

Animals The *Sepp1*-deleted mice were produced by homologous recombination with genomic DNA cloned from a Sv-129 P1 library [21]. All animal studies were approved by the Committee for Animal Studies at our Institute. See the electronic supplementary material (ESM) for further details.

Measurement of selenium Total selenium concentrations were determined using a modification of Watkinson's method [22, 23]. See the ESM for further details.

SEPP1 promoter assay The human *SEPP1* promoter region was cloned to a luciferase reporter vector, and luciferase activities were measured using the dual luciferase assay system (Promega, Madison, WI, USA) [20]. See the ESM for further details.

Cell proliferation assay HUVECs were quantified using Cell Counting Kit-8 (Wako, Osaka, Japan). See the ESM for further details.

Migration assay HUVECs were seeded in the upper chamber of polycarbonate filters, and the number of cells migrating across the filter was counted. See the ESM for further details.

Cell tubule formation assay HUVECs were seeded on plates coated with ECMatrix gel. Endothelial tubule formation was photographed under a microscope. See the ESM for further details.

Matrigel plug implantation assay This assay was performed using a directed in vivo angiogenesis assay inhibition kit (Trevigen, Gaithersburg, MD, USA). See the ESM for further details.

Western blot analysis HUVECs were pretreated with SeP for 24 h. After 2 h of starvation, HUVECs were stimulated with VEGF for 15 min. See the ESM for further details.

RNA preparation and quantitative real-time Real-time PCR was performed on an ABI-Prism 7900HT (Applied Biosystems, Carlsbad, CA, USA). See the ESM for further details.

Reactive oxygen species generation Intracellular reactive oxygen species (ROS) levels were measured using 2′,7′-dichlorofluorescein diacetate (DCF) and quantified using a fluorescent plate reader (Fluoroskan Ascent FL, Yokohama, Japan). See the ESM for further details.

Purification of SeP SeP was purified from human plasma using conventional chromatographic methods [14, 24]. See the ESM for further details.

Preparation of human SEPP1 plasmids and overexpression of SeP in mice The human *SEPP1* expression plasmids were provided by Kaketsuken (The Chemo-Sero-Therapeutic Research Institute, Tokyo, Japan). Plasmid was injected into the tail vein of mice. See the ESM for further details.

Measurement of serum human SeP in mice injected with human SEPP1 plasmid Serum levels of human SeP were measured by enzyme-linked immunosorbent assays using two monoclonal antibodies [15, 25].

Mouse wound healing model Full-thickness wound was created, and the extent of wound closure was examined. See the ESM for further details.

Hindlimb ischaemia model Mice underwent ligation and segmental resection of the left femoral vessel [26]. See the ESM for further details.

Identification of $CD31^+$ vessels An antibody to CD31 was used for immunostaining. See the ESM for further details.

Calculations and statistical analysis All data were analysed using SPSS version 11.0 (Japanese Windows Edition; SPSS, www.ibm.com/software/analytics/spss/). See the ESM for further details.

Results

Glucose increases gene expression and transcriptional activity for SeP in cultured hepatocytes To confirm the elevation of SeP in the livers of people and animal models with type 2 diabetes [15], we examined the action of glucose on *Sepp1* expression in H4-II-EC hepatocytes (Fig. 1). *Sepp1* mRNA expression was significantly increased by 25 mmol/l glucose in a time-dependent manner (Fig. 1a). Additionally, *SEPP1* promoter activity as measured by luciferase activity was increased by 25 mmol/l glucose compared with mannitol (Fig. 1b). These results are consistent with our previous findings showing that treatment with high glucose increases protein levels of SeP in mouse primary hepatocytes [15]. These results indicate that high concentrations of glucose increase the transcriptional activity of SeP genes in the cultured hepatocytes.

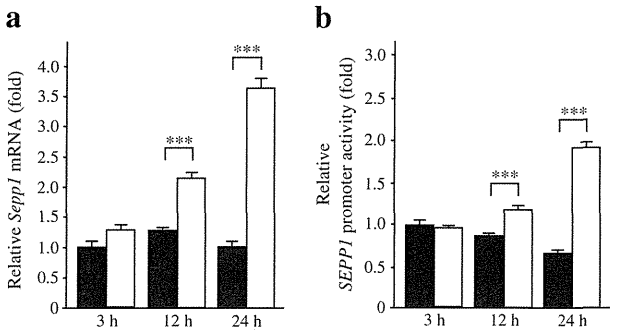

Fig. 1 Glucose increases gene expression and transcriptional activity for SeP in H4-II-EC3 hepatocytes. (**a**) Relative *Sepp1* mRNA expression normalised to β-actin. (**b**) Promoter activity for *SEPP1* in H4-II-EC3 hepatocytes treated with glucose and mannitol. Data are mean ± SD, $n=3$, ***$p<0.001$. White bars, glucose; black bars, mannitol

SeP impairs VEGF-induced angiogenesis in endothelial cells To assess the direct action of the liver-derived secretory protein SeP on vascular endothelial cells, we treated HUVECs with purified human SeP protein. HUVECs were treated with 5 or 10 μg/ml purified human SeP protein, corresponding to serum levels of SeP in healthy individuals or people with type 2 diabetes [15]. In addition, we confirmed that levels of selenium were undetectable (less than 2.5 ng/ml) in all the culture media used for HUVECs. VEGF-induced proliferation of HUVECs was significantly suppressed by treatment with 10 μg/ml SeP (Fig. 2a). Co-administration of buthionine sulfoximine (BSO), an inhibitor of glutathione synthesis, partly rescued the suppressive effect of SeP.

Next, we examined the effects of SeP on VEGF-induced migration in HUVECs. VEGF promoted the migration of HUVECs across polycarbonate filters. This migration was inhibited by the addition of SeP in a concentration-dependent manner (Fig. 2b, c). In the absence of VEGF, treatment with SeP did not affect the migration of HUVECs, suggesting that SeP modulates VEGF-dependent migration of endothelial cells. We further examined the effects of SeP on tubule formation in HUVECs. HUVECs cultured on Matrigel containing VEGF showed morphological tubule formation, with a lumen surrounded by endothelial cells adhering to one another (Fig. 2d). SeP inhibited tubule formation of HUVECs in a concentration-dependent manner (Fig. 2d–e). These in vitro results indicate that SeP at physiological concentrations impairs VEGF-dependent angiogenesis of vascular endothelial cells.

SeP reduces VEGF-stimulated formation of new vessels in Matrigel The role of SeP in angiogenesis in vivo was further determined by Matrigel plug implantation assay. Matrigel was mixed with VEGF in the presence or absence of SeP protein and the plugs were implanted into the dorsal subcutaneous tissue of mice. After 10 days, angiogenesis inside the Matrigel was quantified. SeP markedly inhibited VEGF-stimulated

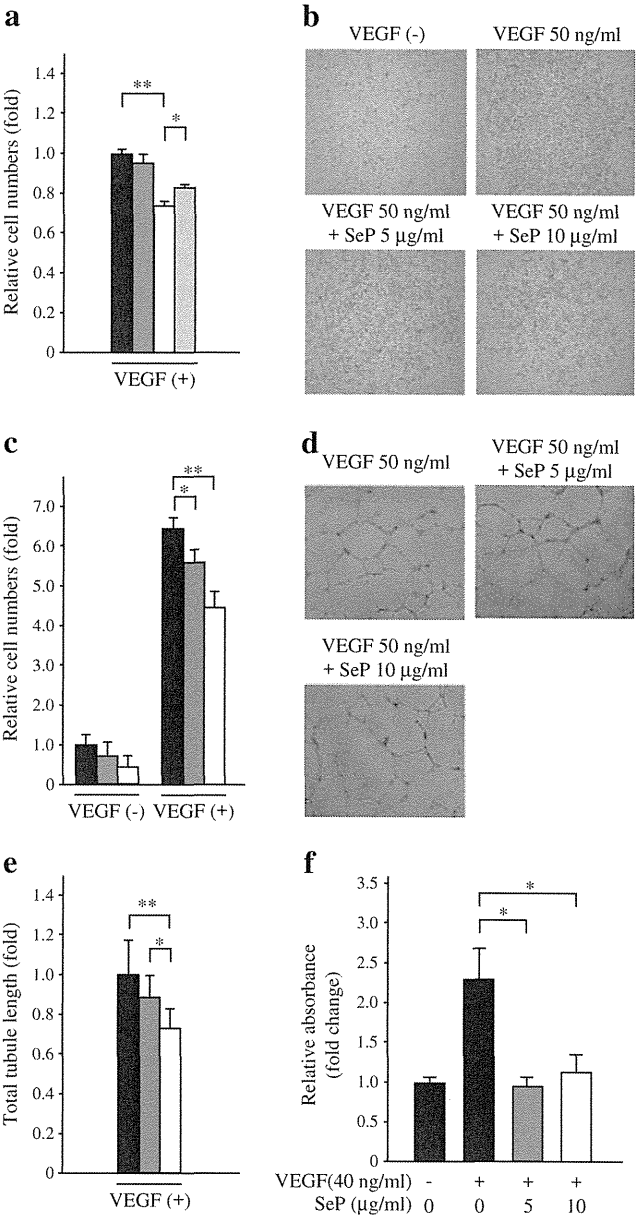

Fig. 2 SeP suppresses VEGF-stimulated angiogenesis in vascular endothelial cells. (**a**) Cell proliferation in HUVECs treated with VEGF for 48 h ($n=12$). (**b**) Representative images of HUVECs that migrated across the polycarbonate filters (magnification×200). (**c**) Quantification of HUVECs that migrated across the filters ($n=8$). (**d**) Representative images of HUVECs that were subjected to Matrigel tubule formation assay (magnification×400). (**e**) Quantification of total tubule length of HUVECs ($n=9$). (**f**) Matrigel implant assay in mice ($n=6$–8). Data are mean ± SEM, *$p<0.05$ and **$p<0.01$. Black bars, control; dark-grey bars, SeP 5 μg/ml; white bars, SeP 10 μg/ml; light-grey bars, SeP 10 μg/ml and BSO 0.2 mmol/l

formation of new vessels in the Matrigel (Fig. 2f). These results further indicate that SeP impairs angiogenesis in vivo.

SeP impairs VEGF signal transduction in endothelial cells Next, we determined whether SeP affects VEGF signal transduction in endothelial cells. Pretreatment with SeP

impaired VEGF-stimulated phosphorylation of VEGF receptor (VEGFR)2 (Tyr1175) and extracellular signal-regulated kinase 1/2 (ERK1/2) (Thr202/Tyr204) in HUVECs (Fig. 3a, b). Co-administration of BSO partially rescued the inhibitory effect of SeP on VEGF signalling (Fig. 3a, b). The mRNA expression of *VEGFR2* (also known as *KDR*) in HUVECs was unaffected by treatment with purified human SeP protein (Fig. 3c). These results indicate that SeP at physiological concentrations impairs VEGF signal transduction in vascular endothelial cells.

SeP suppresses VEGF-induced acute generation of ROS in HUVECs To clarify the mechanism by which the antioxidative protein SeP impairs VEGF signalling, we assessed the action of SeP on the acute generation of ROS stimulated by VEGF. The VEGF-induced ROS burst is reported to be required for the subsequent VEGF signal transduction [27]. Stimulation with 50 ng/ml VEGF for 5 min significantly increased intracellular levels of ROS in HUVECs (Fig. 3d). Pretreatment with SeP suppressed intracellular levels of ROS both with and without VEGF stimulation (Fig. 3d). These results suggest that SeP-induced VEGF resistance is associated with a reduction in the ROS burst stimulated by VEGF.

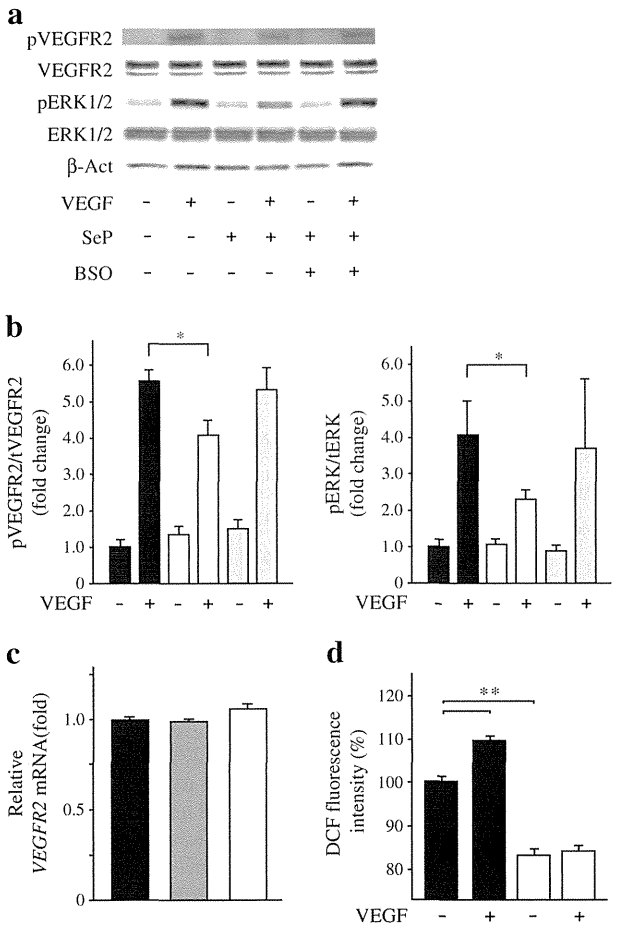

Fig. 3 SeP impairs VEGF signal transduction in endothelial cells. (**a**) VEGF signalling in HUVECs treated with SeP (10 μg/ml). (**b**) Quantification of phosphorylated VEGFR2 and ERK normalised to total VEGFR2 and total ERK in HUVECs (n=6). (**c**) Gene expression levels for *VEGFR2* in HUVECs treated with SeP for 24 h normalised to *GAPDH* (n=6). (**d**) ROS levels in HUVECs stimulated with VEGF for 5 min (n=8). ROS levels were measured as DCF fluorescence intensity. Black bars, control; dark-grey bars, SeP 5 μg/ml; white bars, SeP 10 μg/ml; light-grey bars, SeP 10 μg/ml and BSO 0.2 mmol/l. Data are mean ± SEM. *p<0.05 and **p<0.01. WT, wild-type

SeP delays wound healing of skin in mice To clarify whether hepatic overexpression of SeP affects angiogenesis-related disorder in vivo, we used a hydrodynamic injection method to generate mice that overexpress human *SEPP1* mRNA in the liver. Levels of *SEPP1* gene expression in the liver and SeP protein in the blood were significantly elevated in these mice (Fig. 4a, b), whereas serum levels of total selenium in wild-type and SeP-transgenic mice, which were 322.6 ng/ml and 331.0 ng/ml respectively, were not significantly different (Fig. 4c).

We created excisional wounds (10 mm) in the dorsal skin of the mice and quantified the rate of wound healing. Wound closure was significantly impaired in the mice overexpressing *SEPP1* at 3, 5 and 7 days (Fig. 4d, e). In contrast, *Sepp1*$^{-/-}$mice showed an improvement of the wound closure at 9 days compared with the wild-type animals (Fig. 4f, g). These results indicate that the hepatokine SeP delays the wound healing of the skin in mice.

Sepp1-heterozygous-knockout mice show enhanced angiogenesis after hindlimb ischaemia To determine whether attenuation of SeP expression enhances angiogenesis in vivo, we generated hindlimb ischaemia in *Sepp1*$^{+/-}$mice. We previously reported that *Sepp1*-homozygous-knockout mice exhibit enhancement of insulin signalling in skeletal muscle, whereas *Sepp1*-heterozygous-knockout mice show marginal changes in insulin signalling [15]. Hence, we selected *Sepp1*-heterozygous-knockout mice in the present study to assess the direct actions of SeP on the vascular system, independent of insulin signalling. At 5 days after femoral artery ligation, *Sepp1*$^{+/-}$mice showed a significant increase in blood flow compared with wild-type mice (Fig. 5a). This increase continued for 15 days after artery ligation (Fig. 5b). Consistent with these findings, histological examination showed increased vessel density in the hindlimb musculature as determined by immunostaining with anti-CD31 antibody (Fig. 5c, d).

Discussion

The present study indicates that the liver-derived secretory protein SeP impairs angiogenesis both in vitro and in vivo. SeP directly attenuates VEGF signal transduction in vascular

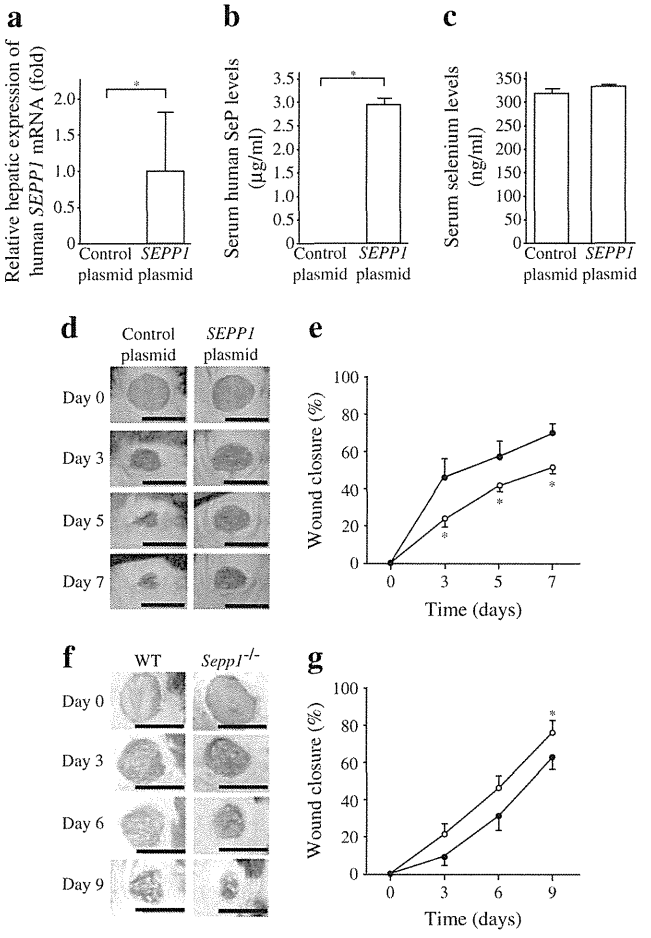

Fig. 4 Hepatic overexpression of SeP impairs wound healing in mice. (**a**) Levels of human *SEPP1* mRNA normalised to 18S rRNA in the livers of mice injected with plasmid DNA via the tail vein (n=9). (**b**) Serum human SeP levels in mice injected with a plasmid encoding *SEPP1* (n=9). (**c**) Serum levels of selenium in mice injected with a plasmid encoding *SEPP1* (n=3). (**d**) Representative images of full-thickness excision rounds on the backs of mice injected with *SEPP1* plasmid. (**e**) Quantification of wound closure in mice injected with *SEPP1* plasmid (white circles) and control (black circles) (n=9). (**f**) Representative images of full-thickness excisional wounds on the backs of *Sepp1*$^{-/-}$mice. (**g**) Quantification of wound closure in *Sepp1*$^{-/-}$mice (white circles) and control (black circles) (n=6–12). Data are mean ± SEM. *p<0.05, scale bars, 10 mm. WT, wild-type

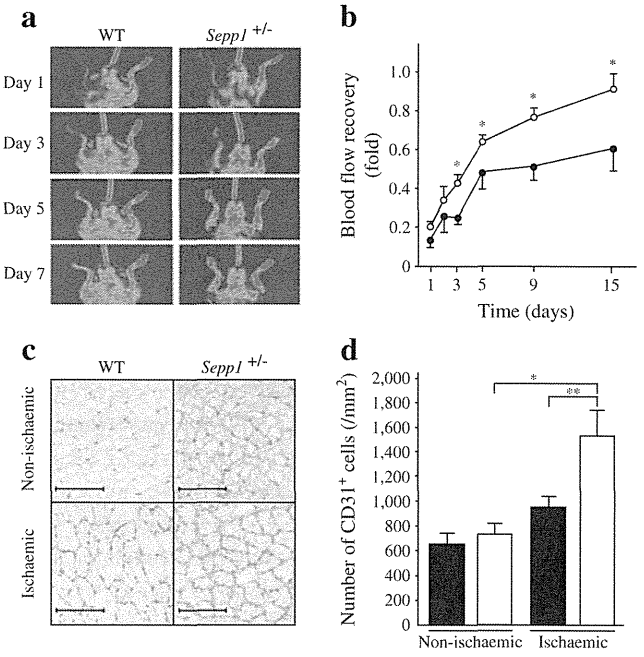

Fig. 5 *Sepp1*$^{+/-}$mice show enhanced angiogenesis during hindlimb ischaemia. (**a**) Representative images of perfusion recovery following hindlimb ischaemia in *Sepp1*$^{+/-}$mice. (**b**) Quantification of blood flow recovery in *Sepp1*$^{+/-}$mice (white circles) and control (black circles) (n=5). Ratios of perfusion from non-ischaemic leg to ischaemic leg are shown. (**c**) Representative images of CD31-stained sections of lower limb tissues of *Sepp1*$^{+/-}$mice at 15 days after ligation. Scale bars 100 μm. (**d**) Quantification of CD31-positive cells in the hindlimb of *Sepp1*$^{+/-}$mice (white bars) and WT (black bars). Data are from 16 fields per section. Data are mean ± SEM. *p<0.05 and **p<0.01

endothelial cells, resulting in suppression of VEGF-induced cell proliferation, migration and tube formation. We reported previously that levels of both hepatic *SEPP1* mRNA and serum SeP protein are elevated in type 2 diabetes [15]. Taken together with our previous report, the present study suggests that hepatic overproduction of SeP may contribute to the onset of impaired angiogenesis in type 2 diabetes (Fig. 6).

The attenuated VEGF signal transduction, VEGF resistance, has been postulated as the molecular mechanism underlying the dysregulation of angiogenesis in people with type 2 diabetes [3, 11]. Waltenberger et al reported that circulating monocytes show attenuation of VEGF-induced chemotaxis in people with diabetes mellitus [28] and that VEGF-stimulated phosphorylation of downstream molecules is reduced in monocytes from patients with type 2 diabetes [29]. In addition, Sasso et al found impaired VEGF signalling in the myocardium of patients with type 2 diabetes and coronary

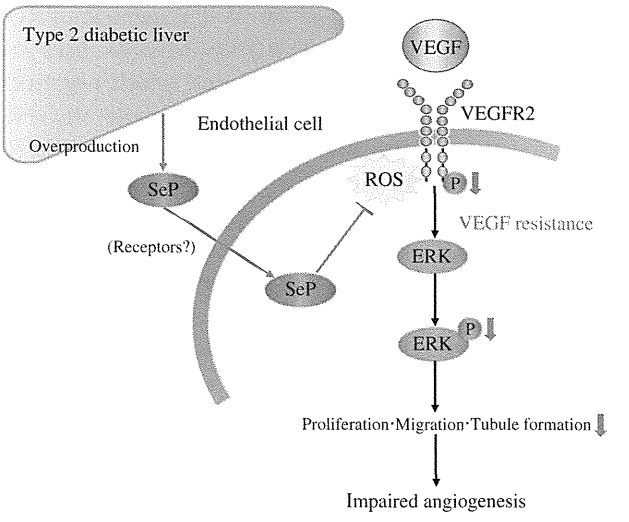

Fig. 6 Overproduction of SeP in type 2 diabetic liver induces VEGF resistance in vascular endothelial cells. SeP inhibits VEGF signal transduction by suppressing acute generation of ROS, resulting in the onset of impaired angiogenesis

heart disease [30], suggesting that diabetes induces VEGF resistance in not only monocytes but also other types of cells such as cardiomyocytes and endothelial cells. However, the molecular mechanisms by which VEGF resistance arises in diabetes mellitus have not been elucidated. The results of the present study suggest a novel molecular pathology of type 2 diabetes; elevation of circulating SeP induces VEGF resistance in vascular endothelial cells.

The liver is the production site of various secretory proteins. Recent work in our laboratory has indicated that genes encoding secretory proteins are abundantly expressed in the liver in type 2 diabetes [31]. Moreover, genes encoding angiogenic factors, fibrogenic factors and redox-associated factors are differentially expressed in the liver in type 2 diabetes, possibly contributing to the pathophysiology and clinical manifestations of this disease [32, 33]. The present study sheds light on a previously under-explored function of the liver; the liver may participate in the regulation of systemic angiogenesis by altering the production of angiogenesis-associated hepatokines such as SeP.

Our observation that SeP impairs angiogenic processes is noteworthy in the context of experimental data suggesting that SeP plays a role in the antioxidative defence system [13]. In fact, we have shown previously that SeP increases the activity of glutathione peroxidase 1 (GPX1), a representative antioxidative enzyme that requires selenium for its enzymatic action, in Jurkat E6-1 cells, a human T cell leukaemia cell line [14]. SeP-induced activation of GPX1 was also demonstrated in endothelial cells [19]. Accumulating evidence indicates that ROS stimulate the angiogenic response in order to initiate the tissue repair process in ischaemia–reperfusion lesions [34]. Among the growth factors involved in angiogenesis, VEGF plays a role in a ROS-dependent signal transduction system [27]. VEGF binding to VEGFR2 stimulates NADPH oxidase in endothelial cells, resulting in the acute generation of ROS such as hydrogen peroxide. This ROS burst oxidises and inactivates protein tyrosine phosphatases, which negatively regulate VEGF signalling and thereby promote VEGFR2 phosphorylation and the subsequent signalling cascade [27].

In combination with these previous reports, the present data suggest that SeP induces VEGF resistance in endothelial cells by increasing GPX1 and subsequently suppressing the VEGF-induced ROS generation that is required for VEGF signal transduction. This speculation was supported by our findings that the co-administration of BSO, an inhibitor of glutathione synthesis, rescued the inhibitory effects of SeP on VEGF signalling and the subsequent VEGF responsiveness. The identification of SeP receptor(s) in endothelial cells would provide further insight into the molecular mechanism by which SeP impairs VEGF signal transduction.

VEGF signalling is known to play paradoxical roles in the pathogenesis of diabetic complications. Both enhancement and suppression of angiogenesis are observed in different tissues in diabetic conditions [35]. In contrast to hindlimb ischaemia or wound healing, advanced diabetic retinopathy is characterised by VEGF-induced abnormal neovascularisation in the retina. Current management for diabetic retinopathy includes anti-VEGF therapy along with blood glucose control [36]. In addition to retinopathy, growing evidence indicates that VEGF-related abnormal angiogenesis plays a major role in diabetic nephropathy [37]. Moreover, a recent report showed that pharmacological inhibition of VEGF-B improves glucose tolerance and insulin resistance in rodent models with type 2 diabetes [38]. Additional studies are needed to determine the actions of SeP on the enhanced angiogenesis in diabetic retinopathy or nephropathy.

Unlike phosphorylation of VEGFR2 and ERK1/2, VEGF-induced phosphorylation of Akt, p38 MAPK and protein kinase, AMP-activated, α1 catalytic subunit (AMPK) was unchanged by SeP in HUVECs (data not shown). Although the detailed molecular mechanism by which SeP selectively impairs VEGFR2/ERK pathway in HUVECs is still unknown, SeP might act on ERK-selective MAPK phosphatases [39]. In fact, some MAPK phosphatases are inactivated by intracellular oxidative stress [39]. However, SeP-induced selective impairment of VEGFR2/ERK pathway should be confirmed in other vascular endothelial cells.

All the culture media we used for HUVECs in this study contained 5.5 mmol/l glucose, which corresponds to fasting plasma glucose levels in people with normal glucose tolerance. However, we confirmed that SeP also attenuated VEGF signalling of HUVECs in the presence of 25 mmol/l glucose (data not shown). These results suggest that SeP induces VEGF resistance in HUVECs in both normoglycaemic and hyperglycaemic conditions. However, additional experiments are clearly needed to determine whether SeP sufficiently removes hyperglycaemia-induced chronic oxidative stress in vascular endothelial cells.

We have shown that serum levels of total selenium were unchanged in the mice injected with *SEPP1* plasmid compared with the control animals (Fig. 4c), in spite of the significant elevation of serum SeP (Fig. 4b). Selenium content in forms other than SeP might decrease in the serum of the SeP-transgenic mice compensatively [14, 40]. Because a recent report showed that SeP exerts antioxidative actions independently of selenium supply [41], we speculate that the phenotype of the SeP-transgenic mice reflects the action of SeP itself, not the abnormal selenium distribution in mice.

Sepp1-heterozygous-knockout mice exhibited an increase in angiogenesis during hindlimb ischaemia without the induction of diabetes (Fig. 5), suggesting that the hepatokine SeP plays a role in the regulation of systemic angiogenesis, irrespective of diabetes status. For example, lipopolysaccharide-induced acute inflammation was reported to downregulate the production of SeP in mice [42]. Angiogenesis promoted by suppressed production of SeP might be beneficial in

inflammatory conditions. Further characterisation of *Sepp1*-deficient mice will provide insights into the involvement of SeP in the regulation of angiogenesis in normoglycaemic conditions.

Serum levels of human SeP in the mice injected with human *SEPP1* plasmid reached approximately 2.0 μg/ml (Fig. 4b). This corresponds with the incremental change in serum level of SeP from that of people with normal glucose tolerance to that of people with type 2 diabetes in the Japanese population [15, 25]. This strongly suggests that the phenotype observed in the SeP-transgenic mice reflects the physiological actions of SeP.

One limitation of the present study is that we examined the action of SeP on endothelial cells only. Various types of cell participate in the angiogenic processes. Further studies are necessary to determine whether SeP exerts effects on other cell types such as the monocytes or endothelial progenitor cells.

Another limitation of the present study is that we carried out all the experiments of *Sepp1*-deficient mice without the induction of diabetes with a high-fat diet or streptozotocin. Hence, we did not investigate the contribution of SeP in the development of the dysregulated angiogenesis seen in diabetes in vivo. However, our data indicate that treatment with purified SeP directly inhibits angiogenesis in both vascular endothelial cells and mice under euglycaemic conditions. Combined with the previous reports showing the elevated production of SeP in type 2 diabetes [15, 16], the current data suggest that overproduction of SeP contributes to the onset of impaired angiogenesis in type 2 diabetes. However, further studies in animals with diabetes are necessary to determine the degree of the contribution of SeP on the impaired angiogenesis observed in diabetes.

In summary, the present study indicates that the diabetes-associated hepatokine SeP impairs angiogenesis by reducing VEGF signal transduction in endothelial cells, and suggests that SeP may be a novel therapeutic target for treatment of VEGF resistance in people with type 2 diabetes.

Acknowledgements We thank M. Wakabayashi, Y. Furuta and Y. Hashimoto of Kanazawa University for technical assistance. We are indebted to K. E. Hill and R. F. Burk of Vanderbilt University School of Medicine for the *Sepp1*-knockout mice.

Some of the data were presented as an abstract at the 9th International Diabetes Federation Western Pacific Region Congress, 4th Scientific Meeting of the Asian Association for the Study of Diabetes, 24–27 November 2012, Kyoto, Japan, and at the 49th annual meeting of the European Association for the Study of Diabetes, 23–27 September 2013, Barcelona, Spain.

Funding This work was supported by Grants-in-Aid from the Ministry of Education, Culture, Sports, Science and Technology, Japan.

Duality of interest The authors declare that there is no duality of interest associated with this manuscript.

Contribution statement KI researched the data and wrote the manuscript. HM conceived and designed the experiments, researched the data, contributed to the discussion, wrote the manuscript and reviewed and edited the manuscript. MK researched the data, contributed to the discussion and reviewed and edited the manuscript. HT, NM-N, NTaj, KC, FL, HA, TO, MS, YT, KK, AF and KM designed the experiments, contributed to the discussion and reviewed the manuscript. YS, YO, YT, KT, HK, SKam and NTak conceived and designed the experiments, researched the data, contributed to the discussion and revised the manuscript critically for important intellectual content. SKan and TT conceived and designed the experiments, contributed to the discussion, wrote the manuscript and reviewed and edited manuscript. TT is the guarantor of this work, has full access to all the data in the study and takes responsibility for the integrity of the data and accuracy of the data analysis. All the authors have approved the final version of the manuscript.

References

1. Holman RR, Paul SK, Bethel MA, Matthews DR, Neil HA (2008) 10-year follow-up of intensive glucose control in type 2 diabetes. N Engl J Med 359:1577–1589
2. Gerstein HC, Miller ME, Byington RP et al (2008) Effects of intensive glucose lowering in type 2 diabetes. N Engl J Med 358:2545–2559
3. Simons M (2005) Angiogenesis, arteriogenesis, and diabetes: paradigm reassessed? J Am Coll Cardiol 46:835–837
4. Abaci A, Oguzhan A, Kahraman S et al (1999) Effect of diabetes mellitus on formation of coronary collateral vessels. Circulation 99:2239–2242
5. Yarom R, Zirkin H, Stammler G, Rose AG (1992) Human coronary microvessels in diabetes and ischaemia. Morphometric study of autopsy material. J Pathol 166:265–270
6. Al-Delaimy WK, Merchant AT, Rimm EB, Willett WC, Stampfer MJ, Hu FB (2004) Effect of type 2 diabetes and its duration on the risk of peripheral arterial disease among men. Am J Med 116:236–240
7. Hueb W, Gersh BJ, Costa F et al (2007) Impact of diabetes on five-year outcomes of patients with multivessel coronary artery disease. Ann Thorac Surg 83:93–99
8. Galiano RD, Tepper OM, Pelo CR et al (2004) Topical vascular endothelial growth factor accelerates diabetic wound healing through increased angiogenesis and by mobilizing and recruiting bone marrow-derived cells. Am J Pathol 164:1935–1947
9. Boodhwani M, Sellke FW (2009) Therapeutic angiogenesis in diabetes and hypercholesterolemia: influence of oxidative stress. Antioxid Redox Signal 11:1945–1959
10. Jude EB, Eleftheriadou I, Tentolouris N (2010) Peripheral arterial disease in diabetes–a review. Diabet Med 27:4–14
11. Waltenberger J (2009) VEGF resistance as a molecular basis to explain the angiogenesis paradox in diabetes mellitus. Biochem Soc Trans 37:1167–1170
12. Carlson BA, Novoselov SV, Kumaraswamy E et al (2004) Specific excision of the selenocysteine tRNA[Ser]Sec (Trsp) gene in mouse liver demonstrates an essential role of selenoproteins in liver function. J Biol Chem 279:8011–8017
13. Burk RF, Hill KE (2005) Selenoprotein P: an extracellular protein with unique physical characteristics and a role in selenium homeostasis. Annu Rev Nutr 25:215–235
14. Saito Y, Takahashi K (2002) Characterization of selenoprotein P as a selenium supply protein. Eur J Biochem/FEBS 269:5746–5751
15. Misu H, Takamura T, Takayama H et al (2010) A liver-derived secretory protein, selenoprotein P, causes insulin resistance. Cell Metab 12:483–495

16. Yang SJ, Hwang SY, Choi HY et al (2011) Serum selenoprotein P levels in patients with type 2 diabetes and prediabetes: implications for insulin resistance, inflammation, and atherosclerosis. J Clin Endocrinol Metab 96:E1325–E1329
17. Arteel GE, Franken S, Kappler J, Sies H (2000) Binding of selenoprotein P to heparin: characterization with surface plasmon resonance. Biol Chem 381:265–268
18. Burk RF, Hill KE, Boeglin ME, Ebner FF, Chittum HS (1997) Selenoprotein P associates with endothelial cells in rat tissues. Histochem Cell Biol 108:11–15
19. Steinbrenner H, Bilgic E, Alili L, Sies H, Brenneisen P (2006) Selenoprotein P protects endothelial cells from oxidative damage by stimulation of glutathione peroxidase expression and activity. Free Radic Res 40:936–943
20. Takayama H, Misu H, Iwama H et al (2013) Metformin suppresses expression of the selenoprotein P gene via an AMPK-FoxO3a pathway in H4IIEC3 hepatocytes. J Biol Chem
21. Hill KE, Zhou J, McMahan WJ et al (2003) Deletion of selenoprotein P alters distribution of selenium in the mouse. J Biol Chem 278:13640–13646
22. Watkinson JH (1966) Fluorometric determination of selenium in biological material with 2,3-diaminonaphthalene. Anal Chem 38:92–97
23. Abdulah R, Miyazaki K, Nakazawa M, Koyama H (2005) Low contribution of rice and vegetables to the daily intake of selenium in Japan. Int J Food Sci Nutr 56:463–471
24. Saito Y, Hayashi T, Tanaka A et al (1999) Selenoprotein P in human plasma as an extracellular phospholipid hydroperoxide glutathione peroxidase. Isolation and enzymatic characterization of human selenoprotein p. J Biol Chem 274:2866–2871
25. Saito Y, Watanabe Y, Saito E, Honjoh T, Takahashi K (2001) Production and application of monoclonal antibodies to human selenoprotein P. J Health Sci 47:346–352
26. Luttun A, Tjwa M, Moons L et al (2002) Revascularization of ischemic tissues by PlGF treatment, and inhibition of tumor angiogenesis, arthritis and atherosclerosis by anti-Flt1. Nat Med 8:831–840
27. Ushio-Fukai M (2007) VEGF signaling through NADPH oxidase-derived ROS. Antioxid Redox Signal 9:731–739
28. Waltenberger J, Lange J, Kranz A (2000) Vascular endothelial growth factor-A-induced chemotaxis of monocytes is attenuated in patients with diabetes mellitus: a potential predictor for the individual capacity to develop collaterals. Circulation 102:185–190
29. Tchaikovski V, Olieslagers S, Bohmer FD, Waltenberger J (2009) Diabetes mellitus activates signal transduction pathways resulting in vascular endothelial growth factor resistance of human monocytes. Circulation 120:150–159
30. Sasso FC, Torella D, Carbonara O et al (2005) Increased vascular endothelial growth factor expression but impaired vascular endothelial growth factor receptor signaling in the myocardium of type 2 diabetic patients with chronic coronary heart disease. J Am Coll Cardiol 46:827–834
31. Misu H, Takamura T, Matsuzawa N et al (2007) Genes involved in oxidative phosphorylation are coordinately upregulated with fasting hyperglycaemia in livers of patients with type 2 diabetes. Diabetologia 50:268–277
32. Takamura T, Sakurai M, Ota T, Ando H, Honda M, Kaneko S (2004) Genes for systemic vascular complications are differentially expressed in the livers of type 2 diabetic patients. Diabetologia 47:638–647
33. Takamura T, Misu H, Matsuzawa-Nagata N et al (2008) Obesity upregulates genes involved in oxidative phosphorylation in livers of diabetic patients. Obesity 16:2601–2609
34. Maulik N, Das DK (2002) Redox signaling in vascular angiogenesis. Free Radic Biol Med 33:1047–1060
35. Costa PZ, Soares R (2013) Neovascularization in diabetes and its complications. Unraveling the angiogenic paradox. Life Sci 92:1037–1045
36. Gupta N, Mansoor S, Sharma A et al (2013) Diabetic retinopathy and VEGF. Open Ophthalmol J 7:4–10
37. Nakagawa T, Kosugi T, Haneda M, Rivard CJ, Long DA (2009) Abnormal angiogenesis in diabetic nephropathy. Diabetes 58:1471–1478
38. Hagberg CE, Mehlem A, Falkevall A et al (2012) Targeting VEGF-B as a novel treatment for insulin resistance and type 2 diabetes. Nature 490:426–430
39. Patterson KI, Brummer T, O'Brien PM, Daly RJ (2009) Dual-specificity phosphatases: critical regulators with diverse cellular targets. Biochem J 418:475–489
40. Deagen JT, Beilstein MA, Whanger PD (1991) Chemical forms of selenium in selenium containing proteins from human plasma. J Inorg Biochem 41:261–268
41. Kurokawa S, Eriksson S, Rose KL et al (2014) Sepp1(UF) forms are N-terminal selenoprotein P truncations that have peroxidase activity when coupled with thioredoxin reductase-1. Free Radic Biol Med 69:67–76
42. Renko K, Hofmann PJ, Stoedter M et al (2009) Down-regulation of the hepatic selenoprotein biosynthesis machinery impairs selenium metabolism during the acute phase response in mice. FASEB J 23: 1758–1765

Case Reports in Ophthalmology

Case Rep Ophthalmol 2014;5:60–65

DOI: 10.1159/000360392
Published online: February 20, 2014

1663–2699/14/0051–0060$39.50/0
www.karger.com/cop

Karger Open access

Topical Treatment for Orbital Capillary Hemangioma in an Adult Using a β-Blocker Solution

Ken Ohnishi[a] Mizuki Tagami[a] Eiichi Morii[b] Atsushi Azumi[a]

[a]Ophthalmology Department, Kobe Kaisei Hospital, Kobe, and [b]Department of Pathology, Osaka University Graduate School of Medicine, Suita (Japan)

Key Words
Orbital capillary hemangioma · Topical treatment · Timolol maleate · Adult case

Abstract
Purpose: To report a case of orbital capillary hemangioma in an adult who was successfully treated with topical timolol maleate 0.5% solution. ***Methods:*** Case report. ***Results:*** A 43-year-old female presented both superficial and deep orbital capillary hemangioma. Topical timolol maleate was applied twice daily. The superficial lesions have nearly disappeared after 1 year of treatment. The deeper lesions have also been reduced in size according to MRI. ***Conclusion:*** We report an adult patient with a relatively large orbital capillary hemangioma who was successfully treated with a topical β-blocker solution. This treatment might be applicable for orbital capillary hemangiomas, regardless of the patient's age, because of its effectiveness and safety.

Introduction

Capillary hemangioma is a common benign vascular tumor of childhood. Within the ocular region, it normally begins on the eyelid but can occasionally occur in the orbit [1]. Histologically, it is characterized by proliferating endothelial cells. It generally appears within a few weeks after birth and undergoes a rapid proliferating phase, followed by a period of quiescence, regressing after a few years into an involution phase [2].

Rootman [3] classified these lesions based on the level of involvement (superficial, subcutaneous, deep orbital, or combined). Capillary hemangiomas of the eyelid and orbit have also been categorized according to their size. Schwartz et al. [4] reported that half of the cases involving hemangiomas with a widest diameter of ≥1 cm would require treatment.

Mizuki Tagami
3-11-15, Shinohara-kitamachi, Nada-Ku
Kobe, Hyogo 6570068 (Japan)
E-Mail m-tagami@kobe-u.ac.jp

Case Rep Ophthalmol 2014;5:60–65
DOI: 10.1159/000360392

Possible acceptable indications for medical intervention include rapidly enlarging lesions, obstruction of the visual axis, significant induced astigmatism and cosmetic concerns. The modalities currently available include intralesional and systemic steroids, bleomycin, interferon-α, topical timolol maleate, oral propranolol, laser treatment and surgical excision [5–10].

We report the case of capillary hemangioma in an adult, which is rare, who was successfully treated with topical timolol maleate 0.5% solution. To our knowledge, this is the first reported application of timolol maleate for an orbital capillary hemangioma in an adult.

Case Report

A 43-year-old female was admitted to hospital with a complaint of bleeding from the right medial ocular angle. She had had a long history of capillary hemangiomas, as described below.

She had developed capillary hemangiomas of the right upper eyelid at the age of 4 and of the right buccal region at the age of 9. Both of those lesions were surgically excised at the time of development. She had also developed a right orbital tumor at the age of 13, which was monitored without any treatment. She presented at the age of 34 with a complaint of right proptosis with ocular pain due to the right orbital tumor, which was confirmed to be an orbital capillary hemangioma after being pathologically diagnosed from an endoscopic biopsy at that time. In the biopsy sample, a lot of dilated capillaries were observed in the mucosa (fig. 1a, arrows), indicating that the lesion was a capillary hemangioma/malformation, but not infantile hemangioma. Radiation therapy and surgical excision were considered but rejected due to a risk of visual loss since the lesion was too close to the optic nerve. Fortunately, the right proptosis with ocular pain had almost disappeared 2 months later with no treatment other than the biopsy. She was then observed without any treatment for years.

Her best-corrected visual acuity was 1.2 OD and 1.5 OS, and the intraocular pressure was 12 mm Hg in both eyes. Slit-lamp examination revealed no abnormalities except the superficial lesions of the capillary hemangioma of her right eye. No abnormalities were found in the retinas of either eye.

The hemangioma presented both superficial and deep orbital components. The superficial lesion was seen at the right medial ocular angle, that is, on the upper/lower eyelids, conjunctiva and expanding into the subconjunctival space. It appeared as superficial tortuous blood vessels, and the conjunctiva appeared violet/blue in color (fig. 1b–d). The deeper lesion lay posterior to the orbital septum and was detected using MRI with low signal intensity on T1-weighted images versus high signal intensity on T2-weighted images with internal signal void (fig. 2a, arrows) and gadolinium enhancement.

The patient was instructed to apply an ophthalmic solution of timolol maleate 0.5% twice daily. The superficial lesion gradually regressed, as shown in fig. 3a–c, and had almost disappeared after 1 year of treatment (fig. 3d). The deeper lesion had also reduced in size, with maximal MRI axial dimensions of 16 × 11 mm (fig. 2a), decreasing to 12 × 8 mm (fig. 2b, arrow) after 1 year of treatment. No apparent recurrence of bleeding in her eye was observed. No local or systemic adverse effects were noted.

Discussion

In recent years, propranolol has yielded encouraging results for capillary hemangioma and is becoming a standard treatment [7]. However, systemic propranolol therapy in children has been associated with a significant incidence of adverse effects such as bronchospasm, bradycardia, hypotension and hypoglycemia [11]. The markedly low rate of adverse reactions to topical timolol maleate treatment reported thus far suggests that it is a safer alternative to systemic propranolol [10, 12].

Our case demonstrated that topical timolol maleate can be delivered effectively to the superficial lesions of capillary hemangiomas in adult patients. It is also effective for the deeper components of capillary hemangiomas to some extent. A further interesting point is that β-blockers are effective not only during the early phase in infants but also in the mature structure of capillary hemangiomas in adults.

Little is known regarding the working mechanism of non-selective β-blockers in the treatment of capillary hemangiomas. Capillary hemangiomas consist of a complex mixture of various types of cells [13]. Immature endothelial cells coexist with immature pericytes, and angiogenic peptides, such as basic fibroblast growth factor and vascular endothelial growth factor, induce proliferation of these immature cells, eventually developing into capillary hemangiomas [13]. β-blockers could potentially influence the signal transduction pathway of these angiogenic factors by modulating the β-adrenergic receptor system, which would explain their effect during the proliferative phase [14]. Other studies demonstrate that non-specific β-blockers are able to trigger apoptosis in capillary endothelial cells in adult rat lung tissue [15]. A similar mechanism might be applicable to the endothelial cells of hemangiomas. Our case suggests that β-blockers can treat capillary hemangiomas even after the completion of tumor growth.

In conclusion, we report the rare case of an adult patient with a relatively large orbital capillary hemangioma who was treated successfully with topical timolol. Topical β-blocker solutions might be applicable to orbital capillary hemangiomas, regardless of the patient's age, because of their effectiveness and safety. Several unresolved issues remain such as the appropriate duration of treatment and the risk of recurrence. A further follow-up of the patient and research on other adults treated with topical timolol for capillary hemangiomas are necessary.

References

1 Shields JA: Vasculogenic tumors and malformations. Capillary hemangioma; in Shields JA (ed): Diagnosis and Management of Orbital Tumors. Philadelphia, WB Saunders, 1989, pp 124–128.
2 Haik B, Karcioglu Z, Gordon RA, Pechous BP: Capillary hemangioma (infantile periocular hemangioma). Surv Ophthalmol 1994;38:399–426.
3 Rootman J: Diseases of the Orbit. Philadelphia, JB Lippincott, 1988, pp 539–543.
4 Schwartz SR, Blei F, Ceisler E, et al: Risk factors for amblyopia in children with periocular capillary hemangiomas of the eyelid and orbit. J AAPOS 2006;10:262–268.
5 Wasserman BN, Medow NB, Homa-Palladino M, Hoehn ME: Treatment of periocular capillary hemangiomas. J AAPOS 2004;8:175–181.
6 Weiss AH, Kelly JP: Reappraisal of astigmatism induced by periocular capillary hemangioma and treatment with intralesional corticosteroid injection. Ophthalmology 2008;115:390–397.
7 Haider KM, Plager DA, Neely DE, et al: Outpatient treatment of periocular infantile hemangiomas with propranolol. J AAPOS 2010;14:251–256.
8 Leaute-Labreze C, Dumas de la Roque E, Hubiche T, et al: Propranolol for severe hemangiomas of infancy. N Engl J Med 2008;358:2649–2654.
9 Elsas FJ, Lewis AR: Topical treatment of periocular capillary hemangioma. J Pediatr Ophthalmol Strabismus 1994;31:153–156.